Review article

In vivo biomarkers of structural and functional brain development and aging in humans

K. Franke[a,*], P. Bublak[a], D. Hoyer[a], T. Billiet[b], C. Gaser[a,c], O.W. Witte[a], M. Schwab[a]

[a] *Department of Neurology, Jena University Hospital, Jena, Germany*
[b] *ICOMETRIX, Leuven, The Netherlands*
[c] *Department of Psychiatry, Jena University Hospital, Jena, Germany*

A B S T R A C T

Brain aging is a major determinant of aging. Along with the aging population, prevalence of neurodegenerative diseases is increasing, therewith placing economic and social burden on individuals and society. Individual rates of brain aging are shaped by genetics, epigenetics, and prenatal environmental. Biomarkers of biological brain aging are needed to predict individual trajectories of aging and the risk for age-associated neurological impairments for developing early preventive and interventional measures. We review current advances of *in vivo* biomarkers predicting individual brain age. Telomere length and epigenetic clock, two important biomarkers that are closely related to the mechanistic aging process, have only poor deterministic and predictive accuracy regarding individual brain aging due to their high intra- and interindividual variability. Phenotype-related biomarkers of global cognitive function and brain structure provide a much closer correlation to age at the individual level. During fetal and perinatal life, autonomic activity is a unique functional marker of brain development. The cognitive and structural biomarkers also boast high diagnostic specificity for determining individual risks for neurodegenerative diseases.

1. Introduction

Endeavors to prolong the healthy lifespan have a long history and have always inspired mankind. With the population aging worldwide, understanding the biology of healthy aging is more relevant than ever. With the great heterogeneity of health outcomes in older individuals (Lowsky et al., 2014), the raised life expectancy prompts fears of an increase in age-related brain diseases such as cognitive decline and dementia (Vos et al., 2012). A major goal of health care systems is to ensure that increased longevity is also accompanied by increased disease-free life expectancy. Effective and affordable strategies are needed to deal with the rising burden of age-related diseases which include a large proportion of neurocognitive and neuropsychiatric disorders (Christensen et al., 2008).

In general, aging is a vastly complex process, broadly defined as a time-dependent decline of organ functions that is driven by the progressive accumulation of cellular damage (Lopez-Otin et al., 2013) and changes in intercellular communication throughout life (Laplante and Sabatini, 2012; Rando and Chang, 2012). Aging is influenced by genetic factors, which itself are modified by environmental epigenetic influences that already have major effects early during development

(Gluckman et al., 2008; Tarry-Adkins and Ozanne, 2014; Van den Bergh, 2011). Biological systems with a long development and/or intrinsic plasticity, such as the central nervous system, the stress axis, and the digestive, cardiovascular and immune systems are especially susceptible to environmental challenges (Bale, 2015; Griffiths and Hunter, 2014; Harris and Seckl, 2011). The plasticity of these biological systems is highest during early development when organ systems are still immature. During critical and sensitive periods of development, early environmental influences act through epigenetic modifications of the DNA, such as DNA methylation, histone modification, and transcriptional regulation by micro RNA, thus allowing optimal adaptation of the organism to its environment (Cao-Lei et al., this issue).

More specifically, structural brain development and aging is characterized by region-specific and non-linear patterns of highly coordinated and sequenced events of progressive (e.g., cell growth and myelination) and regressive (e.g., synaptic pruning) processes during development (Silk and Wood, 2011) and wide-spread atrophy during aging (Good et al., 2001; Resnick et al., 2003). These demonstrate robust patterns of brain structural alterations during development and aging, with some brain regions showing greater alterations than others (Hogstrom et al., 2013; Storsve et al., 2014). Advanced brain aging has

widely been shown to be associated with an increased prevalence of neurodegenerative diseases. With the advent of non-invasive methods of *in vivo* brain imaging, especially magnetic resonance imaging (MRI), and the availability of various automated computational methods for processing and analyzing MRI data, cross-sectional as well as longitudinal neuroimaging studies on brain structure and function are increasingly contributing to a better understanding of healthy as well as aberrant structural brain development and aging.

These changes in brain structure have been shown to be accompanied by changes in cognitive function (i.e., cognitive ageing). During adulthood, performance decline in the majority of cognitive domains and memory impairments occur (Horn and Cattell, 1967), although the precise relationship between structural brain aging and cognitive ageing is still unclear (Hedden and Gabrieli, 2004). However, cognitive processing capacity has been shown to considerably change across the lifespan, gradually declining with increasing age (Baltes et al., 1999; Barrouillet and Camos, 2012). Especially the cerebral system underlying visual perceptual speed and visual short-term memory storage permeate the scaffolding of cognition at all hierarchical levels of the brain (Petersen and Posner, 2012).

Major environmental challenges during the prenatal period include nutrition restriction and stress and have been shown to permanently modify the function of physiological systems, such as the stress axis and the individual trajectory of brain development (Antonelli et al., 2017; Desplats, 2015; Malter Cohen et al., 2013). Increased activity of the stress axis leads to elevated cortisol levels and stress sensitivity. Amongst other effects, increased cortisol levels affect the activity of neurotransmitters such as serotonin and dopamine (Ventriglio et al., 2015; Wyrwoll and Holmes, 2012) and thereby increase the risk for psychiatric illnesses, such as autism spectrum disorders, attention deficit hyperactivity disorder (ADHD), depression, and schizophrenia (Franke et al., this issue; Rose'meyer, 2013; van den Bergh et al., this issue). Changes in the trajectory of brain development have previously been shown by means of several parameters such as brain growth and volume, neuronal structure and metabolism, and inter-neuronal connectivity (Antonelli et al., 2017; Buss et al., 2012; Davis et al., 2013; Desplats, 2015; Favaro et al., 2015; Frodl and O'Keane, 2013; Malter Cohen et al., 2013; Negron-Oyarzo et al., 2016; Pardon and Rattray, 2008; Qiu et al., 2013; Scheinost et al., 2017). Furthermore, changes in the trajectory of brain development have been found to be associated with altered behavior and cognitive function during the entire lifespan (van den Bergh et al., this issue), with early cognitive decline in the elderly (de Rooij et al., 2010), and with increased susceptibility for psychiatric and neurodegenerative diseases (Debnath et al., 2015; Faa et al., 2014). Prenatal stress also leads to reduced adult hippocampal neurogenesis (Belnoue et al., 2013), especially during older age (Koehl et al., 2009). Decreased adult hippocampal neurogenesis is furthermore associated with early cognitive decline and neurodegenerative diseases such as Alzheimer's disease (AD) (Penazzi et al., 2016; Vivar, 2015). Prenatal stress or glucocorticoid exposure also disturbs expression of microtubules and microtubule-associated proteins, which are important for the formation and maturation of neuronal processes (Antonow-Schlorke et al., 2003; Penazzi et al., 2016; Schwab et al., 2001). Abnormal formation of microtubule-associated proteins, for example tau proteins, play a major role in neurodegenerative diseases, such as AD, Parkinson's disease (PD), frontotemporal dementia and other tauopathies (Baird and Bennett, 2013; Pellegrini et al., 2017; Penazzi et al., 2016; Zhang et al., 2016). Furthermore, exposure to inappropriately high levels of cortisol increases susceptibility of neurons to oxidative stress-induced cell death and increased mitochondrial dysfunction, thus accelerating cellular aging during later life (Ahlbom et al., 2000; Debnath et al., 2015; Koehl et al., 2009; Mutsaers and Tofighi, 2012; Simmons, 2012; Tarry-Adkins and Ozanne, 2014). In addition, depressive disorders, for which prenatal stress was shown to increase the risk (van den Bergh et al., this issue), occur more frequently during older age and may be associated with accelerated biological aging at

the cellular and even various systemic levels (Rizzo et al., 2014b; Sodhi et al., 2012; Yatham et al., 2009). Taken together, epigenetic changes during early development represent extremely important determinants of brain development and aging and for the occurrence of age-related brain diseases (Cao-Lei et al., this issue).

To establish preventive measures for age-related brain diseases, it is vital to determine and to predict the individual's status and trajectory of neuroanatomical and cognitive aging, which is shaped by the interaction between genes, environment and life burden over time (Lopez-Otin et al., 2013; Rando and Chang, 2012). Those biological parameters were defined that they "either alone or in some multivariate composite will, in the absence of disease, better predict functional capability at some late age, than will chronological age" (Baker and Sprott, 1988). More specifically, biomarkers of aging have to fulfill several criteria, i.e., it changes with age, has a high individual specificity, is linked to basic mechanisms of aging, correlates with aging and age-related disease (Mather et al., 2011; von Zglinicki and Martin-Ruiz, 2005), has to be both heritable (Nordfjall et al., 2005; Prescott et al., 2011) and modifiable by environmental factors (Huda et al., 2007). Similarly to the development of markers that are aimed to track biophysiological aging (for a recent review see Jylhava et al., 2017), the development of markers tracking the state of neuroanatomical and cognitive aging is enjoying increasing popularity in neuroscience. Determination of the brain age and cognitive age – as opposed to the chronological age – would allow to (1) predict individual neurocognitive performance during different stages of live, (2) identify an individual's health and risk patterns for age-related brain diseases, (3) identify protective or harmful environmental influences on mental health, and (4) apply preventive and interventional strategies that are tailor-made for certain ages (Bocklandt et al., 2011).

More specifically, existing personalized biomarkers of structural and functional brain aging either identify deviations from pre-established reference curves for healthy brain aging or distinguish patients with brain disorders from healthy controls (Arbabshirani et al., 2017; Cohen et al., 2011; Gabrieli et al., 2015; Varoquaux and Thirion, 2014). At the structural level, most of these methods are MRI-based and use state-of-the-art machine learning techniques to establish the reference model for a given task (e.g., healthy aging, disease progression) and to subsequently decode the characteristics of test individuals. At the functional level, cross-sectional studies in different age cohorts and longitudinal studies over restricted time ranges have focused on changing neurocognitive measures across the lifespan, both in childhood and during older age (Deary et al., 2013; McAvinue et al., 2012). With regards fetal brain development, neither MR imaging nor neurocognitive assessments are very feasible. However, fetal behavior, including heart rate patterns (HRP), is directly controlled by age-related brain activity and follows a clear maturational trajectory (Nijhuis et al., 1982; Pillai and James, 1990). Thus, non-invasively recorded HRPs have been shown to provide essential information on fetal functional brain development (Hoyer et al., 2017).

Importantly and in contrast to common group-based classification approaches, regression-based predictive analyses aim to predict the values of continuous variables, such as (regional) brain volume, cognitive, or neuropsychological characteristics (Cohen et al., 2011). Thus, individualized biomarkers of brain development and aging derived from these regression analyses are able to provide valuable and quantifiable parameters that offer a broad range of implementations. Examples include generating reference curves for healthy brain maturation and aging, predicting individual trajectories of brain development and aging based on the pre-established reference curves, and disentangling age-related changes from disease-related changes in brain structure and function.

Here, we review the current state of development of biomarkers determining the structural and functional brain age at the single subject level during different life stages: in the fetal stage, during childhood, adolescence, adulthood, and old age. First, the two most widely used

molecular markers of general biological age and their potential for predicting the individual trajectory of brain development and aging are discussed, i.e. telomere length (Section 2.1) and epigenetic clock (Section 2.2). Then, biomarkers more closely related to brain structure and function are being discussed, which determine prenatal brain development and are based on fetal autonomic analysis (Section 3), structural brain age from childhood into old age, based on MRI (Section 4), and cognitive age in adulthood, based on neurocognitive measures (Section 5).

2. Molecular markers of general biological aging

2.1. Telomere length

An important aspect of individual biological aging is cellular aging. Telomeres shorten with repeated cell divisions that a cell undergoes during its life caused by the incomplete replication of the telomere ends. Telomeres shorten rapidly in infants after birth and during the first years of life (Eisenberg, 2011; Lindqvist et al., 2015). Thereafter, the rate of telomere shortening slows down and remains relatively constant until it further decreases during old age (Mather et al., 2011; Muezzinler et al., 2013; Sanders and Newman, 2013). Once telomeres reach a critically short length, cells are unable to replicate further and DNA cannot be repaired, triggering a persistent DNA damage response and leading a cell to enter a state of irreversible proliferate arrest known as cellular senescence (Campisi and d'Adda di Fagagna, 2007). Cellular senescence has been shown to closely relate to aging and age-related diseases (Bhatia-Dey et al., 2016; Tacutu et al., 2011). Thus, telomere length (TL) is a widely discussed indicator of cellular aging (Blackburn, 2000; Blackburn et al., 2006; Mather et al., 2011). Due to its easy accessibility, TL in humans has been particularly well studied in leukocytes (LTL). TL fulfils several criteria for a biomarker of aging, i.e., it changes with age, has a high individual specificity, is linked to basic mechanisms of aging, correlates with aging and age-related disease, and is both, heritable and modifiable by environmental factors (Huda et al., 2007; Mather et al., 2011; Nordfjall et al., 2005; Prescott et al., 2011; von Zglinicki and Martin-Ruiz, 2005). Therefore, TL can potentially represent the general biological age of an individual more precisely than chronological age.

An important characteristic of senescent cells is the increased secretion of pro-inflammatory cytokine, thus causing additional inflammation and aging (Bhatia-Dey et al., 2016). This property of senescent cells might be of special consequence in the brain since neurons are particularly sensitive to pro-inflammatory cytokines (Liu, 2014). It is, however, not clear whether TL in peripheral leukocytes can be used for predicting the trajectory of brain development and aging.

2.1.1. Telomere length, physical health, and mortality

A high proportion of short telomeres is associated with reduction in years of healthy living (Njajou et al., 2009) and increased mortality risk (Bakaysa et al., 2007; Deelen et al., 2014; for review see Eisenberg, 2011; Mather et al., 2011; Muezzinler et al., 2013; Needham et al., 2015b; Rode et al., 2015; Sanders and Newman, 2013), although causality has not been demonstrated. It has been repeatedly shown that on average women have longer telomeres than men (Gardner et al., 2014; Lapham et al., 2015), which might be related to the increased longevity seen in women (Barrett and Richardson, 2011; Jylhava et al., 2017), Additionally, shorter LTL has been linked to age-related somatic diseases including cardiovascular disease, diabetes, and some types of cancer (D'Mello et al., 2015; Haycock et al., 2014; Kong et al., 2013; Scheller Madrid et al., 2016; Weischer et al., 2012; Wentzensen et al., 2011; Willeit et al., 2014; Zhu et al., 2016), whereas general physical health was inconclusively related to TL (for review see Mather et al., 2011). Although TL appears to oscillate over short periods of time, these variations are less pronounced when long-term follow-up measurements are carried out (Chen et al., 2011; Svenson et al., 2011).

2.1.2. Telomere length, psychosocial stress and lifestyle factors

TL already shows high intra-individual variation at birth (Takubo et al., 2002), suggesting that early environmental influences may alter the trajectory of biological aging (Broer et al., 2013; Eisenberg et al., 2017). Telomeres are subject to epigenetic influences, like other mediators that are involved in the association between prenatal stress and health and disease in later life (Aviv, 2012; Cao-Lei et al., this issue). Consequently, it has been suggested that programming of cellular aging may represent a link between adverse intrauterine influences and health during later life (Entringer et al., 2012). First human studies linked prenatal stress to shorter TL in the newborn, adolescent and the elderly (Entringer et al., 2011; Entringer et al., 2013; Marchetto et al., 2016; Rotar et al., 2015). Childhood psychosocial stress was also associated with shorter TL in peripheral leukocytes and buccal cells in most of the studies, persisting over a long-time until older age, thus exemplifying that telomere shortening is non-reversible (Blaze et al., 2015; Naess and Kirkengen, 2015; Puterman et al., 2016). Accumulated adverse experiences in childhood of any kind further increases the likelihood of having short telomeres later in life, suggesting that early stressors have additive effects on TL (Kananen et al., 2010; Puterman et al., 2016). Thus, early-life stress may have a larger effect on telomere shortening than psychosocial stress during adulthood (Puterman et al., 2016; Shalev et al., 2013). Moreover, the experience of stress is by nature subjective and presumably determines how these experiences subsequently affect the individual health (Lindqvist et al., 2015). However, subjective assessments of experienced stress seem to be more closely related to shorter LTL than an objective categorization of stress (Epel et al., 2004; O'Donovan et al., 2012). It is conceivable that stress coping mechanisms might attenuate stress-associated cell aging (Biegler et al., 2012), but this occurrence has not been well studied.

Accelerated LTL shortening can also be induced by a wide range of lifestyle factors such as smoking, alcohol consumption, low physical activity, high body mass index, low socioeconomic status, and a low level of education, (for review see Lindqvist et al., 2015). The majority of lifestyle factors may also exert their effects on LTL via oxidative stress and inflammation, although the effect size is generally weak (Sanders and Newman, 2013).

2.1.3. Telomere length and psychiatric diseases

Some psychiatric disorders, including schizophrenia and depressive disorders, are associated with accelerated biological aging and shorter life expectancy (for an excellent review see Lindqvist et al., 2015) as well as with an increased risk of neurodegenerative diseases such as dementia (Rizzo et al., 2014a). However, studies examining an association of LTL with psychiatric diseases are inconclusive and characterized by a high variability of LTL between individuals and studies (Colpo et al., 2015; Lindqvist et al., 2015). Although the strongest evidence for an association between shortened TL and psychiatric disorders is seen in major depressive disorders (Henje Blom et al., 2015; Lindqvist et al., 2015), telomere shortening in general seems to be increased in chronic or severe disease, after longer disease duration, and at an older age, but does not appear to be related to a specific psychiatric illness (Kananen et al., 2010; Lindqvist et al., 2015; Needham et al., 2015a). Comorbidities and confounds, such as age, medication as well as biological and methodological issues, may possibly explain some of the variability in the findings. Furthermore, comorbidities with secondary psychiatric disorders such as alcohol or substance abuse and confounds such as age and medication may itself be associated with shortened LTL (for review see Lindqvist et al., 2015; Pavanello et al., 2011; Yang et al., 2013). Taken together, present data support the model of accelerated cellular aging as a theoretical explanation for accelerated biological aging and lower life expectancy in psychiatric diseases (Colpo et al., 2015; Lindqvist et al., 2015).

2.1.4. Telomere length, cognitive function and neurodegenerative diseases

Chronological age is the primary risk factor for many

neurodegenerative diseases, including AD, PD, and frontotemporal dementia. A growing body of literature shows that TL is associated with the process of neurodegeneration and has thus been suggested as a biomarker for cognitive aging (for review see Boccardi et al., 2015; Cai et al., 2013; Eitan et al., 2014; Rizvi et al., 2014). Although some studies showed an association between telomere shortening and cognitive impairment (Boccardi et al., 2015; Insel et al., 2012; Jenkins et al., 2006; Valdes et al., 2010), results of studies in AD and PD are inconclusive (Boccardi et al., 2015; Cai et al., 2013; Eitan et al., 2014; Forero et al., 2016a, 2016b; Rizvi et al., 2014; Zekry et al., 2010a, 2010b). This is surprising since oxidative stress and chronic neuroinflammation play essential roles in AD and PD pathogenesis, similar as in telomere shortening (for review see Cai et al., 2013; Tansey and Goldberg, 2010), thus suggesting that oxidative stress-mediated LTL shortening is associated with AD pathogenesis. Additionally, the interaction between environmental factors and genotype may have a specific role in development of AD and TL shortening, e.g. patients that are homozygous for apolipoprotein E (ApoE)-ε4 are at an increased risk for developing AD and have significantly shorter LTL than those, who are heterozygous (Takata et al., 2012). This may be probably due to the ApoE-ε4 protein being a less efficient antioxidant than ApoE-ε3 or ApoE-ε2, thus probably inducing higher oxidative stress in leukocytes of ApoE-ε4 homozygous individuals (Shea et al., 2002). However, cognitively non-impaired individuals with an increased risk for developing AD (i.e. ApoE-ε4 positive) did not show a relationship between LTL or peripheral blood mononuclear cell (PBMC) telomerase activity and hippocampal volume (Jacobs et al., 2014; Wikgren et al., 2012). Additionally, a recent meta-analysis could not show that ApoE genotype was an effect moderator for the relationship between LTL and hippocampal volume (Nilsonne et al., 2015).

Taken together, it is not yet known whether peripheral telomere shortening is associated with AD. Further, it is also not clear, whether TL attrition is causally related to, associated with, or maybe even a consequence of AD. Just as unclear is the potential mechanism linking telomere shortening, amyloid pathology and cognitive impairment. Similarly, the role of telomere shortening in pre-dementia cognitive aging is unknown.

2.1.5. Relationship between telomere length in peripheral leukocytes and in the brain

The discussion on using telomere shortening as biomarker of brain aging focuses on to what extent LTL is a surrogate marker of cellular senescence in brain cells, as telomere shortening in neurons might be restricted to neural stem cells, since mature neurons do not divide (Ferron et al., 2009). In agreement with that, TL estimation in brain tissue without consideration of the cell type showed only weak correlation with LTL at the single subject level (Dlouha et al., 2014; Lukens et al., 2009). Also, TL was shown to vary across brain regions, thus suggesting variable trajectories of cell aging, with hippocampus and substantia nigra having the longest telomeres and the dorsolateral prefrontal cortex having the shortest (Mamdani et al., 2015). Additionally, TL in brain tissue did not show telomere shortening with age (Takubo et al., 2010). Furthermore, a heterogeneous picture for cerebral TL and LTL has been observed in psychiatric and neurodegenerative brain diseases (Mamdani et al., 2015; Szebeni et al., 2014; Zhang et al., 2010).

In agreement with the weak correlation between LTL and TL in brain tissue, the small number of MRI-based studies, which have been performed in healthy subjects to show brain volume decrease as a measure of structural brain aging in relation to telomere shortening, did not find a clear relationship between LTL or PBMC telomerase activity and brain volume (Lindqvist et al., 2015). In accordance with that, the most important population-based study by King et al. (2014) including the largest sample by far with almost 2000 participants, associations between shorter LTL and hippocampus, region-specific, total cerebral and white matter volumes were only small (King et al., 2014).

Similarly, another study in non-demented subjects also found shorter LTL being associated with subcortical volume atrophy (Wikgren et al., 2014).

While AD patients tend to show shorter LTL, only one study conducted in a small number of subjects found evidence of telomere erosion in the AD hippocampus (Franco et al., 2006). In contrast, in another study, telomeres were even longer in hippocampal cells of human AD brains compared to controls, although LTL was shortened (Thomas et al., 2008). A third study showed that TL in the cerebellum of AD patients was similar to that in peripheral leukocytes (Lukens et al., 2009). Thus, even when exclusively examining psychiatric and neurodegenerative diseases, the evidence for an association between peripheral and central telomere erosion and accelerated brain aging is inconclusive.

2.1.6. Integrative perspective on telomere length

In conclusion, shorter LTL in general seems to be associated with increasing age, although correlation coefficients are mostly pretty low. Inconsistent study results may be explained by biological and methodological factors, such as study design, differences amongst study populations, and methods of measurement. Moreover, it still remains unclear whether TL is a biomarker of aging for the whole organism – or a biomarker of aging in specific tissues. Indeed, the widely conflicting results on the value of TL as a biomarker of aging have produced more questions than answers.

Thus far, it has been assumed that peripheral TL erosion is related to life-long cellular proliferative activity as well as to pathophysiological processes, which are common during aging and present in most of age-related diseases, e.g. inflammatory and oxidative stress. However, the relationship between TL erosion and aging has been dispelled by the fact that telomeres do not need to become critically short in order to elicit cellular senescence (Rossiello et al., 2014). Another major problem is the high variability of TL between individuals (Takubo et al., 2002), with TL been found to already vary at birth, depending on genetic, epigenetic, and early environmental factors. In addition, the normal rate of telomere shortening and its biological variance is still unclear. Several factors, such as stress, lifestyle, and therapy, can modulate TL and the rate of telomere shortening. It remains uncertain, whether such modulation really changes the trajectory of aging or obscures any relationship between TL and biological aging (Gomes et al., 2011).

In contrast to the progress that has been made on the use of TL as an estimate for the general biological age, there is less clarity regarding the use of LTL as a reliable biomarker of brain age in particular. Similarly, no reliable conclusions can be drawn at present with regard to LTL as a biomarker for accelerated brain aging in general as well as in neurodegenerative diseases. Studies possibly need to focus more on aging phenotypes than on disease diagnoses. Moreover, the unknown relationship of LTL to TL in brain tissue or other central cell aging markers depicts another major limitation in interpreting existing study results.

In line with the current state of knowledge in the field, the inconsistent study base, and existing results, which lack to show age-associated "normal ranges" for LTL, a recent study did not show any association between TL and MRI-based brain age (Cole et al., 2017c). Consequently, much more basic research is needed to acquire a better understanding of whether LTL shortening is associative to or plays a causal role in accelerated brain aging during normal aging and in brain-related diseases, before LTL might be used as an efficient biomarker for brain aging in future. Further, clinical studies associating peripheral TL with phenotypic markers of brain structure and function are needed, including various forms of neuroimaging and cognitive testing. In future, longitudinal designs will allow investigations into whether LTL shortening precedes brain atrophy, or vice versa. Moreover, studies will need to focus on aging phenotypes, in addition to disease diagnoses.

2.2. Epigenetic clock

The epigenetic clock, i.e. the DNA methylation age (DNAmAge), has been recently identified as a feasible predictor for biological age (for a review see Jylhava et al., 2017). The most popular clock measures show high age correlations and small mean deviations from chronological age. The Horvath's clock is a multi-tissue predictor based on methylation levels of 353 CpG sites and was developed in a sample of n = 8000, aged 0–101 years, resulting in r = 0.96 and a median absolute error of 3.6 years for age prediction (Horvath, 2013). The Hannum's clock uses whole blood samples and is based on only 71 CpG sites and was developed in a sample of n = 656, aged 19–101 years, resulting in r = 0.91 and a root mean squared error (RMSE) of 4.9 years (Hannum et al., 2013). In independent studies, the correlations between both clocks vary from fairly strong (r = 0.76; Chen et al., 2016) to moderate (r = 0.37; Belsky et al., 2016). Observations of men having higher epigenetic ages compared to women are consistent across studies (Hannum et al., 2013; Horvath, 2013; Horvath and Ritz, 2015; Jylhava et al., 2017; Marioni et al., 2016; Marioni et al., 2015a).

2.2.1. Epigenetic age and mortality

In a recent meta-analysis the epigenetic clock showed its ability to predict mortality independent of common risk factors such as age, body mass index (BMI), education, physical activity, alcohol use, and smoking, with epigenetic age estimates incorporating Hannum's clock measures based on blood cell counts outperforming other clock measures in terms of statistically significant associations with all-cause mortality (Chen et al., 2016).

Epigenetic age based on Hannum's clock was a strong predictor for cancer incidence and cancer-related mortality, with results suggesting a dose-responsive relationship between epigenetic age measured in blood, cancer incidence, and mortality: for each one-year increase in the difference between chronological and epigenetic age, risk of developing cancer within three years was increased by 6% and risk of dying of cancer within the next five years was increased by 17% (Zheng et al., 2016). Another study showed better prediction results for all-cause, cancer-related, and cardiovascular-related mortality for epigenetic age based on Horvath's clock (Perna et al., 2016), However, longitudinal studies are needed to evaluate the predictive value of the epigenetic age over time (Jylhava et al., 2017).

2.2.2. Epigenetic age, individual health, and cognition

Epigenetic age based on Horvath's clock in blood cells was also shown to be associated with poorer cognitive and physical fitness in the Lothian Birth Cohort 1936 at age 70 years, but did not predict the rate of change in cognitive and physical fitness during the 6-year follow-up (Marioni et al., 2015b). Also, age-related frailty index – measured as deficits in multiple bodily systems – was found to be directly associated with the Horvath clock in old age (Breitling et al., 2016). In a study with participants aged 25–85 years, a moderate correlation between BMI and epigenetic age acceleration could only be observed in liver tissue, but not in blood, muscle, and adipose tissue. The authors reported an epigenetic age increase by 3.3 years for each 10 BMI units (Horvath et al., 2014). In another study including participants aged 30–100 years, epigenetic ages based on Horvath's as well as Hannum's clock were associated with an increase in BMI and with indicators of diabetes and the metabolic syndrome. However, protective effects of healthy diet, physical exercise, and higher education were only observed for epigenetic age based on Hannum's clock (Quach et al., 2017). Furthermore, HIV as well as Down Syndrome (DS), Huntington's disease (HD), Parkinson's disease were recently found to lead to significantly increases in epigenetic age of brain tissue (HIV: 7.4 years; DS: 11.5 years; HD: 3.2 years), blood (HIV: 5.2 years; DS: 4.6 years), or a combination of brain tissue and blood (DS: 6.6 years) (Horvath et al., 2015; Horvath et al., 2016b; Horvath and Levine, 2015; Horvath and Ritz, 2015). The authors suggest the observed accelerated aging effects

in blood may reflect changes in blood cell composition, but give no conclusive explanation of the observed accelerated aging effects in brain tissue.

In a sample of non-demented participants, aged 63–102 years, epigenetic age at death derived from Horvath's clock in *postmortem* extracted brain cells (specifically, the dorsolateral prefrontal cortex) no association to cognitive functioning and memory up to 16 years before death (mean study time: 4 years) was found (Levine et al., 2015). The authors suggest that the lack of findings might reflect the relatively low variance of cognitive measures among non-demented controls. In middle-aged adults, increased blood-based Hannum's clock, but not Horvath's, was associated with poorer cognitive and physical fitness, health, and facial aging (Belsky et al., 2016), whereas another study in middle-aged monocygotic twins did not find associations between blood-based epigenetic age and cognitive functioning (Starnawska et al., 2017).

Thus, it seems that the epigenetic clock can indeed reflect aging in different bio-physiological domains and across a wide age range, but associations to cognitive domains are inconsistent (Jylhava et al., 2017).

2.2.3. Epigenetic age and neurodegenerative diseases

In longitudinally followed up AD patients (mean follow-up: 4 years), increased epigenetic age at death as derived from Horvath's clock in *postmortem* extracted brain cells (i.e. dorsolateral prefrontal cortex) was associated with a decline in global cognitive functioning, episodic memory and working memory in the years before death, as well as *postmortem* presence of plaques and amyloid load (Levine et al., 2015).

In PD patients, aged 37–91 years (mean ca. 70 years), epigenetic age of the immune system was significantly increased (Horvath and Ritz, 2015). It was thus concluded, that these results support the hypothesis of peripheral immuno-inflammatory characteristics, observed as accelerated aging of blood cells, being involved in PD (Jylhava et al., 2017).

2.2.4. Integrative perspective on the epigenetic clock

In contrast to other molecular markers such as TL, cellular ageing, as measured by the epigenetic clock, moderately to strongly correlate with chronological age, regardless of tissue types. The epigenetic age was also shown to predict all-cause mortality, cancer- and cardiovascular-related mortality, as well as to correlate with cognitive and physical fitness in the elderly, and being able to detect accelerated ageing induced by various factors including obesity, Down syndrome, and HIV infection (for reviews see Gibbs, 2014; Lowe et al., 2016).

To date, it is not entirely clear which aspects of cellular aging the epigenetic clock represent. It is most probably not purely a mitotic clock, since aging has also been shown to be traceable in non-proliferative tissue such as brain (Jylhava et al., 2017). However, rates in epigenetic aging in several tissues were found to differ from one another. It was suggested that epigenetic aging is an intrinsic property of the cells, probably a function of the epigenetic maintenance system, which is uncoupled from cell senescence per se (Horvath, 2013; Lowe et al., 2016). Additionally, it has been suggested that the intrinsic Horvath clock is representing overall frailty in the body, whereas the Hannum's clock may be closer related to immune responses (Horvath and Ritz, 2015; Jylhava et al., 2017).

With regards to other biomarkers, correlations between epigenetic age and TL and other clinical measures have generally been low or non-significant, but were suggested to be associated with age and mortality independent of each other (Belsky et al., 2016; Breitling et al., 2016; Jylhava et al., 2017; Marioni et al., 2016). In addition, the cell-type adjusted Horvath clock has been found to be not associated with common disease risk factors such as alcohol use, smoking, diabetes, hypertension, and the levels of high- and low density lipoproteins, insulin, glucose, triglycerides, C-reactive protein (CRP) and creatinine (Horvath et al., 2016a; Jylhava et al., 2017). Furthermore, with regards

to cognitive functioning and neurodegenerative diseases, associations were thus far only found in *postmortem* brain tissue, but not in blood samples. Thus, the epigenetic clock is actually not suitable to serve as an *in vivo* biomarker for aging of brain structure and function. This is supported by a recent study that showed no association between epigenetic age and MRI-based brain age (Cole et al., 2017c).

3. A biomarker for fetal brain development

3.1. Autonomous activity as functional marker of fetal brain development

Aberrations of fetal brain development may not only influence cognitive ability during the entire life span but may also alter the trajectory of brain aging. They are often induced by environmental challenges such as stress or insufficient fetal nutrient supply (Antonelli et al., 2017; Desplats, 2015; Malter Cohen et al., 2013). Since these challenges are preventable, biomarkers for early aberrations of functional fetal brain development are highly desirable to allow the development and implementation of early preventive or interventional measures. However, the assessment of fetal brain development poses a challenge. At the structural level, only large structural disturbances in brain development such as a hydrocephalus are detectable using MRI. At the functional level, fetal brain activity is assessable by means of magnetoencephalography (MEG) but only averaged evoked responses are detectable due to the small signal amplitude (Kiefer et al., 2008). More appropriate for clinical application is the activity of the autonomic nervous system (ANS), which is associated with the majority of physiological control mechanisms. The functioning of fetal ANS is mainly reflected in the noninvasively recorded heart rate patterns (HRP), which also provides essential information on fetal functional brain development (Hoyer et al., 2017). Fetal behavior such as body movements, eye movements, and HRP is directly controlled by brain activity and follows a clear maturational trajectory (Nijhuis et al., 1982; Pillai and James, 1990).

A more sophisticated understanding of how physiological developmental principles are reflected in fetal behavior might improve the assessment of individual (brain) development. During the ontogenetic period, the development of an organism is based on its genetic code as well as on environmental influences and follows principles of self-organization and adaptation (Fig. 1). Those principles are universal in open non-equilibrium systems in non-living and living natural systems (Bertalanffy, 1968; Kauffman, 1993; Nicolis and Prigogine, 1977). Consequently, they may also have implications for the epigenetic processes involved in fetal programming (Provenzi et al., 2016). In physiological systems, these universal developmental characteristics are increasing fluctuation amplitudes, increasing complexity, and pattern formation. They clearly coincide with fetal HRP during the course of fetal development (Hoyer et al., 2009; Hoyer et al., 2013; Van Leeuwen et al., 1999).

According to the "developmental origins of adult disease (Barker) hypothesis" (Barker, 1998), early identification of aberrations in fetal brain development is the base for timely interventions when the condition is still reversible. An altered trajectory of brain development is associated with an altered maturation of the brain-derived stress system (Charil et al., 2010). The stress system with its two branches, the hypothalamo-pituitary-adrenal (HPA)-axis and the ANS, is highly susceptible to early environmental influences such as prenatal stress or

malnutrition (Antonelli et al., 2017; Desplats, 2015; Malter Cohen et al., 2013). Developmental programming of the activity of the stress system may predispose for aberrations in neurocognitive function and stress-associated diseases such as ADHD and depression (Franke et al., this issue; Rose'meyer, 2013; van den Bergh et al., this issue). Changes in the activity of the HPA axis and the ANS following prenatal stress (Dodic et al., 2002; Rakers et al., 2013; Shaltout et al., 2011) or malnutrition (Frasch et al., 2007; Hawkins et al., 1999; Nijland et al., 2010) are already detectable during fetal life. Notably, activity of the ANS influences HRP (Electrophysiology, 1996). Since the heart rate is one of the few physiological parameters that can be obtained non-invasively from the fetus, HRP analysis is uniquely suited to assess fetal functional brain development and its aberrations (Thayer et al., 2012). Such analyses are of major interest to assess the trajectory of functional brain development and pathophysiological disturbances.

Fetal HRP, as an index of the autonomic (neuro-vegetative) brain activity, reflect the instantaneous autonomic control of various organ systems depending on the behavioral state and individual characteristics such as the maturational state of the ANS and developmental aberrations (Kouskouti et al., 2017). HRP can be monitored starting at around 15 weeks of gestational age (wG) in the prenatal period and subsequently over the entire life span (Electrophysiology, 1996). Heart rate variability (HRV) increases continuously during the prenatal and subsequent postnatal period. During most of childhood, HRV is found to increase as well, and thereafter it decreases from about 20 years of age.

After about 30 wG periods of active and quiet behavior can be distinguished (Nijhuis et al., 1982), leading to fully developed states of sleep and wakefulness in the postnatal period. The high level of agreement between HRP and a comprehensive sleep state classification taking the electroencephalogram, eye movements and body movements into consideration allows a sufficient behavioral state classification only via HRP analysis already in the prenatal period (Nijhuis et al., 1982). While vagal rhythms modulate HRV predominantly during quiet sleep in the fetus, heart rate accelerations of increasing amplitude and duration that mainly reflect maturational increase of sympathetic autonomic activity typically evolve during active sleep (Nijhuis et al., 1982; Pillai and James, 1990). To capture different sleep and behavioral states, a typical HRP recording period needs to last 30 for min, as shown in Fig. 2 (Hoyer et al., 2017).

From the established ultrasound-based cardiotocography (CTG), it is known that fetal heart rate fluctuations increase during the course of pregnancy, and that heart rate deceleration (DC) patterns which are predominant at an earlier gestational age, i.e. at about before 32 wG are replaced by heart rate acceleration (AC) patterns during late pregnancy (DiPietro et al., 1996). In contrast to CTG technology that does not allow for the identification of individual heartbeats, fetal magnetocardiography (fMCG) allows a beat-precise HRV analysis from about 15 wG onwards. Although fetal electrocardiography (fECG) gives more or less corresponding recordings, the signal quality is lower. In particular there is a gap at 28–32 wG when the fetus is almost completely covered and electrically isolated by the vernix caseosa (Hoyer et al., 2017). Those signals reflect the increasing stability and regulatory capacity of the cardiac pacemaker as well as the developing vagal and sympathetic nervous system and autonomic control.

HRV frequency bands can be assigned to vagal and sympathetic heart rate modulations in a simple linear manner (David et al., 2007). This linear approach of frequency band analysis is a fundamental
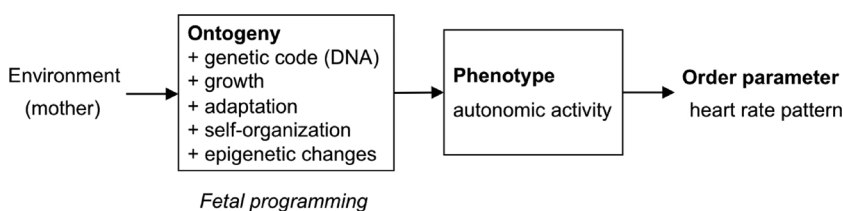

Fig. 1. Ontogenetic development is dependent on internal (fetal) and environmental (maternal) influences. The behavior of the phenotype can be assessed from the behavior of order parameters such as heart rate patterns.
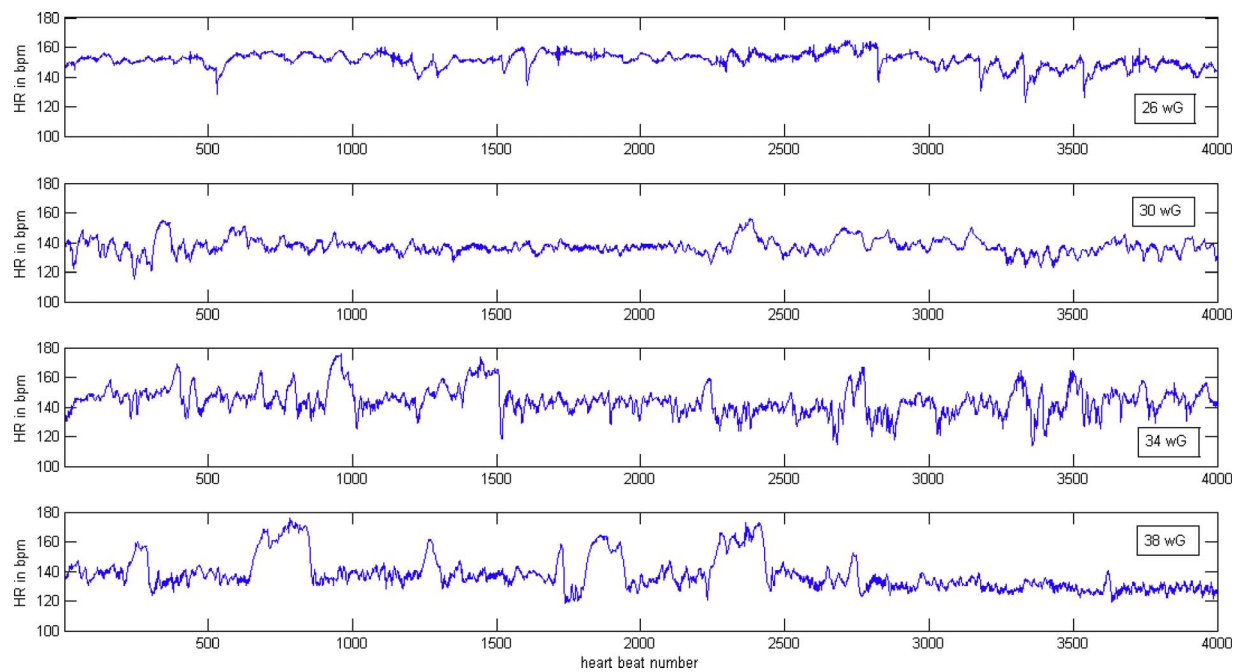
Fig. 2. Fetal tachograms, instantaneous heart rate (HR) over 4000 beats (about 30 min) in dependence on week of gestational age (wG). At 26 wG, heart rate DC (see drops e.g. around beat number 550) dominate, at 30 wG small DC and AC appear, at 34 wG, typical DC no longer appear but clear AC of increasing amplitude dominate (see peaks e.g. around beat number 900, at 38 wG, an active sleep state with distinct AC up to about beat number 2800 is shown followed by a period of quiet sleep characterized by a period of mainly absent AC.
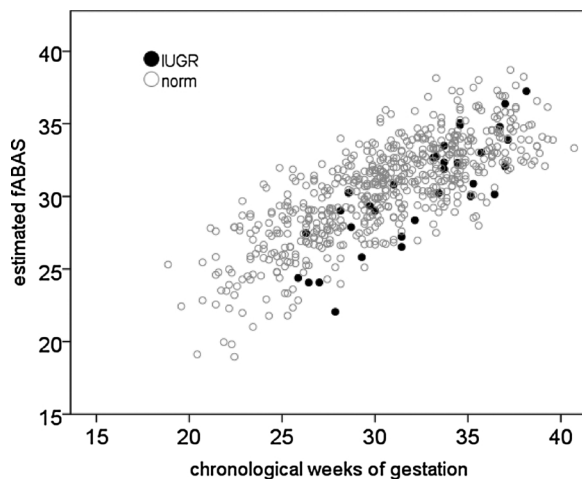

Fig. 3. Functional fetal autonomic brain age score values of 30 min fMCG recordings of a normal population and the reduced values of an IUGR group (Details according to Hoyer et al., 2013).

restriction that neglects the interdependencies between different rhythms such as between vagal and sympathetic activity. Newer approaches, which provide valuable additional information on these physiological interrelationships and behavioral patterns, are more appropriate for the complex nonlinear physiological system. In MCG recordings from about 15 wG onwards, the amplitude of fetal heart rate fluctuations of all frequency bands and the complexity of fetal heart rate fluctuations continuously increase and saturate in the last weeks before term (Van Leeuwen et al., 2003; Van Leeuwen et al., 1999).

The developmental characteristics mentioned above support their usage in a functional fetal autonomic brain age score. HRV indices of fluctuation amplitude, complexity of sympatho-vagal rhythms, and pattern formation (skewness, baseline stability) were used in multivariate regression models that predict the functional maturation age (Hoyer et al., 2014; Hoyer et al., 2013). Models for 30 min recordings without a fetal behavioral state specification, as well as those for

10 min sections of quiet sleep and active sleep were fitted to predict the maturation age of 364 normal cases (20–40 wG) from the Jena Fetal Monitoring Data Base. Functional fetal autonomic brain age score was subsequently validated in external data bases, namely in 322 fetal MCG recordings (15–40 wG) from the Grönemeyer Institute of Microtherapy, Bochum, Germany (Hoyer et al., 2015), and in 358 CTG recordings (24–40 wG) from the Hospital de S. João, University Porto, Portugal (Hoyer et al., 2017) in the respective overlapping ranges of wG. From these studies, we summarize with respect to a precise fetal functional brain age assessment: *(i)* the design of the functional fetal autonomic brain age score was confirmed across study centers and recording technology with low loss of precision, *(ii)* recordings over 30 min are necessary for an appropriate consideration of behavioral statistics, *(iii)* the individual fetal beat detection and a low error rate mainly determine the precision of the developmental age assessment. In fetuses suffering from intrauterine growth restriction (IUGR), HRV amplitude (i.e., sort term variation, STV) and complexity are reduced (Ferrario et al., 2009; Nijhuis et al., 2000). All STV values of the IUGR group were below the median of the normal group nomogram and were distributed around the 2.5 percentile. Functional fetal autonomic brain age score values of IUGR fetuses were found reduced both in the Jena and the Bochum MCG study centers mentioned above (Hoyer et al., 2015; Hoyer et al., 2013), as shown for the Jena data set in Fig. 3 in data neglecting the fetal sleep state.

We conclude that universal developmental characteristics are reflected in HRP during the course of prenatal development. They allow an evaluation of the functional maturation age of autonomic function as well as developmental disturbances. The standard error of autonomic brain age assessment in healthy fetuses older than 15 wG is below 3 wG, which is smaller than the reduction of values assessed in IUGR fetuses (Hoyer et al., 2013). The analysis of further clinical data of fetal stress is pending. The main limitations for a direct assessment of the developmental age of the fetal brain include the high cost and local setting of fMCG devices. Furthermore, cross validation studies on different HRV indices and fetal developmental disturbances are lacking. In contrast, fetal routine CTG is standardized for *intrapartum* fetal monitoring. And consequently, knowledge and dissemination structures exist with respect to the early identification of developmental problems of fetuses

based on HRV indices. Further optimization and complimentary validation of HRV indices across fMCG, fECG, and CTG technologies and their relationship to developmental disturbances is currently the subject of international research. Yet the present results of selected applications already indicate the potential for the early identification of developmental disturbances, which might have implications for improving prenatal care in clinical practice.

4. MRI-based biomarkers for structural brain development and aging

4.1. MRI-based markers

Changes in brain structure throughout the lifespan have multi-dimensional aspects, which can be covered and quantified by several MRI modalities, realized by using diverse MR pulse sequences and protocols as well as a variety of analytical techniques for processing MRI data. These data may result in several different markers for the individual brain structure that are sensitive to and capture shared as well as marker-specific information on (age-related) brain tissue changes (Cherubini et al., 2016; Groves et al., 2012). The most widely used modality is T1-weighted MRI, providing a number of parameters, including voxel-wise, regional and global gray matter (GM) and white matter (WM) volumes, volumetric data for subcortical regions, cortical thickness, and cortical surface area. Complementary measures of individual brain characteristics provide information about the myelin content and white matter integrity in regions of interest (ROIs) and fiber tracts (from T2-weighted MRI), the mineralization of subcortical nuclei (from T2* relaxometry), and information about fiber density, axonal diameter, myelination in white matter, as well as several measures of water diffusion in brain tissue (from diffusion tensor imaging; DTI). For a short overview of the different modalities and resulting parameters please refer to Table 1.

4.2. Modeling structural brain development and aging

A growing body of research uses high-dimensional neuroimaging data, often including several hundred (multi-modal) parameters per individual, and employing supervised, linear or non-linear pattern recognition techniques in order to depict and quantify structural brain development and aging across the lifespan. In contrast to univariate approaches, multivariate analyses of individual brain structure are capable of detecting and quantifying subtle and widespread deviations in region- or voxelwise brain structure throughout the whole brain for a given age (for a recent opinion paper please see Cole and Franke, 2017).

In general, an age prediction model needs to be trained first in order to subsequently assess a person's individual brain age. The age prediction model is generated by recognizing multivariate patterns of age-typical brain structure and parameters based on (multi-modal) MRI data from a (large) sample of cognitively healthy subjects. Subsequently, the age prediction model is applied in previously unseen test subjects, estimating the individual brain ages based on their (multi-modal) MRI data. The difference between a person's estimated brain age and chronological age finally identifies individuals deviating from the typical brain development and/or aging trajectory.

A growing number of non-invasive MRI-based brain age biomarkers have recently been introduced. These biomarkers reliably and validly model healthy brain development (Section 4.3) and aging (Section 4.4), integrating and/or comparing different *(i)* types of neuroimaging data, *(ii)* image pre-processing pipelines, *(iii)* feature selection techniques, and *(iv)* pattern recognition algorithms. In order to generate and validate the brain age model, most of the studies employ a "cross-validation" approach, i.e., the neuroimaging parameters of a large proportion of the reference sample of healthy individuals is used to generate the brain age model first. The generated brain age model is then applied to the smaller proportion of the reference sample that was not included in

Table 1
Overview of modalities and derived parameters used for brain age prediction in this review.

Model	Tool	Modality	Parameter	Explanation
Structural brain age	MRI (magnetic resonance imaging)	T1-weighted	GM	Gray matter volume/density throughout the brain (per voxel, region, or global)
			WM	White matter volume/density throughout the brain (per voxel, region, or global)
			Subcortical volumes	Volumetric data for subcortical regions
			Cortical thickness	Thickness of cortical gray matter
			Cortical surface area	Expansion of area of cerebral cortex surface
		T2-weighted	Signal intensities	Signal intensity in white matter regions and fiber tracts, associated with myelin content and white matter integrity; recognizing white matter hyperintensities
		T2* relaxometry	R2* (relaxation rates)	Reflecting mineralization of the subcortical nuclei
		DTI (diffusion tensor imaging)	FA (fractional anisotropy)	Presence of preferred direction of diffusion (i.e. tissue anisotropy), reflecting fiber density, axonal diameter, and myelination in white matter
			MD (mean diffusivity)	Amount of all isotropic diffusion (i.e. not bounded by membranes), measuring the average molecular motion independent of any tissue directionality
			AD (axial diffusivity)	Amount of isotropic diffusion along direction of maximal diffusion
			RD (radial diffusivity)	Amount of isotropic diffusion perpendicular to direction of maximal diffusion
		DWI (diffusion weighted imaging)	ADC (apparent diffusion coefficient)	Amount of diffusion along applied gradient direction, reflecting magnitude of diffusion (of water molecules) within tissue
Fetal brain age	MCG (magnetocardiography)	Fetal HRP (heart rate patterns)	DC-AC development	Change in deceleration (DC) & acceleration (AC) patterns
Cognitive brain age	TVA (theory of visual attention)	Perceptual threshold		Rate of information uptake (i.e., numbers of elements processed per sec)
		Processing speed		
		VSTM storage capacity		Storage capacity in visual short-term memory
		VSTM processing rate		Processing rate in visual short-term memory

model generation (i.e., "left-out"), in order to predict individual brain ages based on the neuroimaging parameters. This procedure is repeated multiple times, until an individual brain age is provided for each subject in the reference sample. Some of the studies described in this review additionally include independent test samples of healthy and clinical subjects and even MRI scanners, in order to prove the generalizability of the pre-established brain age model across different samples, and for broad application in a clinical context, respectively.

The total number of subjects used to generate a brain age model has recently been identified as the single most important factor driving prediction accuracy (Franke et al., 2010). Although most of the studies generating models for healthy brain development and aging utilize large and often publicly available study samples, the specific compositions of the samples and number of subjects used to generate the brain age models differ between studies, which complicates comparison of the prediction accuracy and results between the different models. To evaluate the various studies with regard to prediction accuracy, practicality in further research and clinical contexts, and generalizability, we report all available data on the samples used to generate and validate the different brain age models, i.e., the age ranges covered, the number of MRI scanners used (incl. field strengths), the MRI modalities and parameters acquired, the mathematical algorithms adopted to model healthy brain development and aging, the cross-validation plans applied to test the algorithm, as well as several measures for the accuracy of brain age predictions, including Pearson's correlation coefficients (r) between individual brain age and chronological age, mean absolute error (MAE), and root mean squared error (RMSE):

$$MAE = 1/n * \Sigma_i |BA_i - CA_i|, \qquad (1)$$

$$RMSE = [1/n * \Sigma_i (BA_i' - CA_i)^2]^{1/2}, \qquad (2)$$

with n being the number of subjects in the test sample, BA_i the subject's predicted brain age, and CA_i the subject's chronological age.

4.3. Review of studies predicting brain age during development

To our knowledge, seven studies establishing models for brain development covering age ranges between early childhood and young adulthood have been published so far (Table 2; Brown et al., 2012; Cao et al., 2015; Dosenbach et al., 2010; Erus et al., 2015; Franke et al., 2012b; Khundrakpam et al., 2015; Wang et al., 2014). Accuracies for brain age predictions derived from cross-validation in the whole reference sample of healthy subjects ranged from $r = 0.43$–0.96 and MAEs from 1.03–1.95 years.

The most accurate model for brain age prediction during development in healthy individuals aged 3–20 years used a number of parameters derived from different MRI modalities (i.e., T1, T2, DTI), including cortical thickness, cortical surface area, subcortical volumes, apparent diffusion coefficient, fractional anisotropy, and T2 signal intensities in predefined subcortical regions, applying a *regularized multivariate nonlinear regression-like approach* with *leave-one-out cross-validation*, resulting in $r = 0.96$ and MAE = 1.03 years (Brown et al., 2012). Although each single MRI modality showed similar predictive power ($r \approx 0.9$) across the full age range (i.e., 3–20 years), modality-specific contributions to the generation of the brain age model differed across neuroanatomical structures and age sub-ranges: "At the youngest ages, from about 3–11 years old, measures of T2 signal intensity within subcortical ROIs were by far the strongest predictors of developmental phase, declining in importance through the early teens. Diffusion measures within white matter fiber tracts, in comparison, were consistently strong predictors across the age range, becoming the highest contributor during the middle ages of about 12–15 years. T1-derived morphological measures varied, with cortical thickness and subcortical volumes contributing more than cortical area, which was consistently the weakest predictor over age. Interestingly, diffusivity measures within subcortical ROIs increased sharply at about age 14 and were the

strongest maturational predictors at the oldest ages, from about 17–20 years old." (Brown et al., 2012, p. 3). Additionally, modality-specific subsets showed worse prediction accuracies compared to the combined model (T1 subset: $r = 0.91$, MAE = 1.71 years; T2 subset: $r = 0.91$, MAE = 1.60 years; DTI subset: $r = 0.90$, MAE = 1.71 years). Erus et al. (2015) also used a number of parameters derived from different MRI modalities (i.e., T1, DTI), generating and testing their brain age model by utilizing *linear support vector regression (SVR)* with *10-fold cross-validation* in a sample of healthy individuals aged 8–22 years. Again, the combined model ($r = 0.89$, MAE = 1.22 years) proved to be more accurate than single parameter measures (i.e., apparent diffusion coefficient: $r = 0.85$, MAE = 1.35 years; fractional anisotropy: $r = 0.83$, MAE = 1.41 years; GM: $r = 0.81$, MAE = 1.52 years; WM: $r = 0.76$, MAE = 1.71 years; CSF: $r = 0.43$, MAE = 2.71 years). However, both studies did not incorporate an independent test sample to prove generalizability of the generated brain age model.

Using only a single MRI modality, the most accurate model utilized voxelwise GM and WM volume derived from T1-weighted MRI, generating and testing their brain age model by utilizing *linear relevance vector regression (RVR)* with *leave-one-out cross-validation* in a sample of healthy individuals aged 5–19 years, resulting in $r = 0.93$, MAE = 1.2 years (Franke et al., 2012b). Furthermore, it outperformed all other brain age models using only a single MRI modality or single-modality subsets, and additionally proved sufficient generalizability across different scanners and even across studies, utilizing two independent test samples ($r = 0.89$, MAE = 0.5 years & $r = 0.75$, MAE = 1.1 years).

4.4. Review of studies predicting brain age during adulthood

To our knowledge, 20 studies establishing models for brain aging, covering age ranges from early to late adulthood have been published so far (Table 3; Ashburner, 2007; Cherubini et al., 2016; Cole et al., 2015; Franke et al., 2010; Groves et al., 2012; Han et al., 2014; Kandel et al., 2013; Konukoglu et al., 2013; Liem et al., 2017; Lin et al., 2016; Mwangi et al., 2013; Neeb et al., 2006; Sabuncu and Van Leemput, 2011; Sabuncu et al., 2012; Schnack et al., 2016; Steffener et al., 2016; Tian et al., 2016; Wang and Pham, 2011; Wang et al., 2014). Accuracies for brain age predictions derived from cross-validation in the whole reference sample of healthy subjects ranged from $r = 0.43$–0.97, MAEs from 4.3–13.5, and RMSEs from 5.1–21.0 years.

Regarding modeling of healthy brain aging during adulthood into senescence, studies mathematically modeling healthy brain aging, which use a number of parameters derived from different MRI modalities, tended to provide more accurate brain age predictions. Groves et al. (2012) generated a model of normal brain aging utilizing a sample of healthy subjects aged 8–85 years. This model was based on a number of T1- and DTI-derived parameters, generating and testing by utilizing *linked independent component analysis (ICA)* with *leave-one-out cross-validation*, resulting in an overall prediction accuracy of $r = 0.97$ and MAE = 5.9 years. Cherubini et al. (2016) also used a number of parameters derived from different MRI modalities (i.e., T1, T2, T2*, DTI), generating and testing their brain age model by utilizing *multiple linear regression* with *leave-one-out cross-validation* in a sample of healthy individuals aged 20–74 years, resulting in an overall age prediction accuracy of $r = 0.96$. Additionally, this study found voxel-wise mean diffusivity to be the main predictor of the brain age model (i.e., explaining 62.4% of intra-individual variance), followed by GM volume (18.3%), T2* (14.2%), and fractional anisotropy (3%). However, both studies neither provided prediction accuracies for single modalities, nor validated their brain age models across scanners or in independent samples.

A very recent study used a number of parameters derived from T1 and T2*, including cortical and subcortical measures as well as connectivity data, generating and testing the brain age model by utilizing *linear support vector regression (SVR)* with *half-split cross-validation* (Liem

Table 2
Models for brain maturation in infants and adolescents using non-invasive structural markers.

Study	Training sample (healthy subjects) No [female]	Age mean ± SD (yrs) [range]	Independent test sample No [female]	Age mean ± SD (yrs) [range]	MRI training [no of scanners]/ MRI test [no of scanners]	Modalities	Quantitative parameters used for brain age modeling	Algorithm for age modeling	Train-Test split for validation	Prediction performance in training sample r	MAE (yrs)	Prediction performance in test sample r	MAE (yrs)
Brown et al. (2012)[a]	885 (48%)	3–20 (13.0 ± 4.9)	–		3T [12]	T1, T2, DTI	Cortical thickness, cortical area, subcortical volumes, diffusivity (tracts), diffusivity (ROIs), signal intensity (tracts), signal intensity (ROIs)[b]	Multivariate non-linear regression	LOO	0.96[b]	1.03[b]	–	
							T1 subset (cortical thickness, cortical area, subcortical volumes)			0.91	1.71		
							T2 subset (signal intensity in tracts & ROIs)			0.91	1.60		
							DTI model (diffusivity in tracts & ROIs)			0.90	1.71		
Cao et al. (2015)[a]	303 (53%)	5–18 (11.2 ± 3.8)	115 (53%)[c]	7–18 (12.1 ± 3.1)	1.5T [6]/1.5T [6] (same)	T1	GMV per region (cortical & subcortical)	Multivariate linear regression (LASSO)	LOO	0.82	1.69	0.83	1.71
Dosenbach et al. (2010)	238 (48%)[d]	7–30 (18.2 ± 6.7)[e]	195 (52%)[d]	7–31 (16.4 ± 7.1)[e]	3T [1]/ 1.5T [1]	rs-fcMRI	Functional connectivity maps (derived from resting state BOLD time courses for 160 ROIs)	Linear SVR	LOO	0.74	–	0.72	–
			186 (53%)[d]	6–35 (15.3 ± 6.6)[e]	1.5T [1]					–		0.75	–
Erus et al. (2015)[a]	621 (56%)	8–22 (15.1 ± 3.3)	–		3T [1]	T1, DWI, DTI	RAVENS maps for GM, WM, VN; voxelwise maps for ADC & FA[f]	Linear SVR	10-fold CV	0.89[f]	1.22[f]	–	
							ADC			0.85	1.35		
							FA			0.83	1.41		
							GM			0.81	1.52		
							WM			0.76	1.71		
							VN			0.43	2.71		
Franke et al. (2012b)[a,g]	394 (47%)	5–19 (10.7 ± 3.8)[e]	10/15[h]	12–16 (14.5 ± 1.5)	1.5T [6]/1.5T [1] (diff.)	T1	Concatenated GMV & WMV (voxelwise)	Linear RVR	LOO	0.93	1.2	0.89/0.75[h]	0.5/1.1[h]
	341	5–19 (10.7 ± 3.8)[e]	53	5–18 (10.7 ± 4.0)	1.5T [5]/1.5T [1] (diff.)					–		0.95[h]	1.1
	318	5–19 (10.7 ± 3.8)[e]	76	5–18 (10.5 ± 3.8)	1.5T [5]/1.5T [1] (diff.)							0.92	1.2
	323	5–19 (10.5 ± 3.7)[e]	71	5–19 (11.8 ± 4.1)	1.5T [5]/1.5T [1] (diff.)							0.92	1.3
	319	5–19 (10.7 ± 3.7)[e]	75	5–18 (10.4 ± 4.0)	1.5T [5]/1.5T [1] (diff.)							0.93	1.2
	346	5–19 (10.8 ± 3.8)[e]	48	5–18 (9.8 ± 3.8)	1.5T [5]/1.5T [1] (diff.)							0.91	1.3
	324	5–19 (10.7 ± 3.9)[e]	70	6–18 (10.8 ± 3.4)	1.5T [5]/1.5T [1] (diff.)							0.90	1.2

Table 2 (continued)

Study	Training sample (healthy subjects)		Independent test sample		MRI training [no of scanners]/ MRI test [no of scanners]	Modalities	Quantitative parameters used for brain age modeling	Algorithm for age modeling	Train-Test split for validation	Prediction performance in training sample		Prediction performance in test sample	
	No [female]	Age mean ± SD (yrs) [range]	No [female]	Age mean ± SD (yrs) [range]						r	MAE (yrs)	r	MAE (yrs)
Khundrakpam et al. (2015)[a,g]	308 (56%)[i]	5–18 (12.9 ± 3.8)	[g]		1.5T [6]	T1, T2, PDW	Cortical thickness per region, for different no of cortical parcels: 78 160 1248 2560 10240	Elastic net penalized linear regression	10-fold CV[k]	0.78 0.81 0.82 0.83 0.84	1.95 1.79 1.74 1.71 1.68	0.77 0.80 0.82 0.82 0.82	1.99 1.82 1.77 1.78 1.76
Wang et al. (2014)[a]	303 (47%)	7–22 (11.8 ± 2.6)	–	–	1.5T [2], 3T [1]	T1	Cortical thickness, mean curvature, Gaussian curvature (all regionwise)	RVR (with Gaussian RBF kernel)	10-fold CV	0.79	1.38	–	

- = data not given or not applicable; ADC = apparent coefficient of diffusion; BOLD = blood oxygen level–dependent; CV = cross-validation; DTI = diffusion tensor imaging; DWI = diffusion weighted imaging; FA = fractional anisotropy; rs-fcMRI = resting-state functional connectivity MRI; FLAIR = fluid-attenuated inversion recovery; GM = gray matter; GMVgrey = grey matter volume; LASSO = least absolute shrinkage and selection operator; LOO = leave-one-out; MAE = mean absolute error between brain age and chronological age; MD = mean diffusity; PDW = proton density-weighted images; RAVENS = regional analysis of volumes examined in normalized space; RBF = radial basis function; ROI = region of interest; SD = standard deviation; SVR = support vector regression; VN = ventricular; WM = white matter; WMV = white matter volume.

(same) Test data were acquired on the same MRI scanner as training data.

(diff) Test data were acquired on a different MRI scanner than training data.

[a] Data from publicly available databases. For more details on the data please refer to the cited paper.

[b] Performance for model including all modalities as input. Performance measures using modality subsets are given below.

[c] Independent test sample formed from follow-up MRI scans 2 years after 1st MRI scan.

[d] This number denotes the number of scans.

[e] Recalculated by the authors of the review paper.

[f] Performance for model including all 5 image maps as input. Performance measures using each image type in isolation are given below.

[g] MRI scanner-site effects were tested, i.e. brain age model was trained on data from 5 sites and tested on the from the left-out site, repeated for each site.

[h] The study included 2 independent test samples.

[i] Longitudinal data is used to model brain aging (n = 679).

[k] All (longitudinal) scans of subject i were either in the training set or in the test set.

Table 3
Models for brain aging during adulthood using non-invasive structural markers.

Study	Training sample (healthy subjects)		Independent test sample		MRI training [no of scanners]/ MRI test [no of scanners]	Modalities	Quantitative parameters used for brain age modeling	Algorithm for age modeling	Train-Test split for validation	Prediction performance in training sample			Prediction performance in test sample	
	No [female]	Age mean ± SD (yrs) [range]	No (female)	Age mean ± SD (yrs) [range]						r	MAE (yrs)	RMSE (yrs)	r	MAE (yrs)
Ashburner (2007)[a]	471 [44%]	32 [17–79]	–		1.5T [1]	T1	GM & WM density maps (small/large deformations)	Linear RVR	400/71 (50×)	0.83/ 0.81[c]	–	7.55/ 7.90[c]	–	–
								RVR, RBF 0.5[b]		0.82/ 0.83[c]	–	7.64/ 7.34[c]		
								RVR, RBF 1[b]		0.84/ 0.85[c]	–	7.07/ 6.84[c]		
								RVR, RBF 2[b]		0.85/ 0.86[c]	–	6.84/ 6.64[c]		
								RVR, RBF 4[b]		0.85/ 0.86[c]	–	6.74/ 6.56[c]		
								RVR, RBF 8[b]		0.86/ 0.86[c]	–	6.70/ 6.52[c]		
								RVR, RBF 16[b]		0.86/ 0.86[c]	–	6.68/ 6.50[c]		
								RVR, RBF 32[b]		0.85/ 0.85[c]	–	6.80/ 6.64[c]		
Cherubini et al. (2016)	140 [58%]	42 ± 14 [20–74]	–		3T [1]	T1, T2, T2*, DTI, FLAIR	GMV, R2*, MD, FA (all voxelwise)	Multiple linear regression	LOO	0.96	–	–	–	–
Cole et al. (2015)[d]	1537 [50%]	42 ± 20 [18–90]	113 [57%]	43 ± 20	1.5T & 3T [> 10]/ 3T [1] (diff.)	T1	Similarity matrix of MRI data for: GMV (voxelwise) / WMV (voxelwise)	GPR	10-fold CV	0.92 / 0.92	6.20 / 6.16	– / –	0.93 / 0.93	5.80 / 6.35
Cole et al. (2017a, 2017b, 2017c, 2017d)[d]	2001 [49%]	40 ± 18 [18–90]	105 [6%]	56 [50–62]	1.5T & 3T [> 10]/ 3T [2] (diff.)	T1	Similarity matrix of MRI data for concatenated GMV & WMV (voxelwise)	GPR	10-fold CV	0.94	5.01	6.31	0.69	–
Franke et al. (2010)[a,d]	547 [56%]	48 ± 17 [19–86]	108 [37%]	32 ± 10 [20–59]	1.5T [2], 3T [1]/ 1.5T [1] (diff.)	T1	GMV (voxelwise)	Linear RVR	400/137 (1x)	0.94	4.61/ 4.96[e]	5.90	0.89	5.44/ 5.57[e]
								ε-SVR (optimized)		–	4.85/ 4.85[e]	–	–	5.42/ 5.51[e]
								ε-SVR (default)		–	9.82/ 4.76[e]	–	–	5.97/ 5.39[e]
								ν-SVR (optimized)		–	4.85/ 4.85[e]	–	–	5.51/ 5.51[e]
								ν-SVR (default)		–	11.06/ 4.72[e]	–	–	6.38/ 5.36[e]
Groves et al. (2012)	484	[8–85]	–		1.5T [1]	T1, DTI	FA, MD, MO, GMV, cortical thickness, cortical surface area	Linked ICA	LOO	0.97	5.9	–	–	–

Table 3 (*continued*)

Study	Training sample (healthy subjects)		Independent test sample		MRI training [no of scanners]/ MRI test [no of scanners]	Modalities	Quantitative parameters used for brain age modeling	Algorithm for age modeling	Train-Test split for validation	Prediction performance in training sample			Prediction performance in test sample	
	No [female]	Age mean ± SD (yrs) [range]	No (female)	Age mean ± SD (yrs) [range]						r	MAE (yrs)	RMSE (yrs)	r	MAE (yrs)
Han et al. (2014)[a,d]	201	[4–85]	–		3T [1]	DTI	Connectivity matrix:	CBR (linear)	Half-split (100x)			–	–	
							- no normalization			0.77	10.41			
							- normalization within subjects			0.68	11.83			
							- normalization between subjects			0.59	14.14			
							- no normalization	CBR (non-linear)		0.79	9.50			
							- normalization within subjects			0.69	11.64			
							- normalization between subjects			0.60	14.39			
							- no normalization	PLSR		0.72	9.80			
							- normalization within subjects			0.67	10.28			
							- normalization between subjects			0.43	13.51			
							- no normalization	ε-SVR (optimized)		0.77	10.26			
							- normalization within subjects			0.63	16.73			
							- normalization between subjects			0.53	15.46			
Kandel et al. (2013)[a]	191[f]	72 ± 8	–		[4]	T1	Cortical thickness	Sparse linear regression	LOO/ 3-fold CV[g]	0.52	3.70/ 5.58[g]	–	–	
								Elastic net (with LASSO)		0.46	3.12/ 5.86[g]	–		
Konukoglu et al. (2013)[a,d]	414	[18–93]	–		1.5T [1]	T1	GMV (voxelwise)	NAF/kNNc for k = 1	LOO	0.91/ 0.86[h]	10.9/ 14.3[h]	–		
								k = 7		0.94/ 0.91[h]	8.6/ 11.9[h]			
								k = 15		0.94/ 0.90[h]	8.5/ 12.2[h]			
								k = 413		0.93/ 0.88[h]	9.7/ 21.0[h]			

Table 3 (*continued*)

Study	Training sample (healthy subjects)		Independent test sample		MRI training [no of scanners]/MRI test [no of scanners]	Modalities	Quantitative parameters used for brain age modeling	Algorithm for age modeling	Train-Test split for validation	Prediction performance in training sample			Prediction performance in test sample	
	No [female]	Age mean ± SD (yrs) [range]	No (female)	Age mean ± SD (yrs) [range]						r	MAE (yrs)	RMSE (yrs)	r	MAE (yrs)
Liem et al. (2017)[d]	2354 [48%]	59 ± 15 [19–82]	475 [65%]	46 ± 19 [18–85]	3T [1]/ 3T [1] (diff.)	T1, T2*	Concatenated matrix including brain connectivity (197 & 444 regions), cortical thickness, cortical surface area, subcortical volumes[i]	Linear SVR	Half-split	0.93[j]	4.29[j]	–	0.86[j]	8.02[i]
							Connectivity matrix 197 & 444			0.89	5.25	–	0.71	11.22
							Connectivity matrix 197			0.87	5.99	–	0.69	11.56
							Connectivity matrix 444			0.88	5.77	–	0.68	11.85
							Cortical & Subcortical measures			0.91	4.83	–	0.87	7.39
							Cortical thickness			0.87	5.95	–	0.79	9.23
							Cortical surface area			0.79	7.29	–	0.47	13.24
							Subcortical volume			0.84	6.44	–	0.81	9.10
Lin et al. (2016)	112 [52%]	67 ± 7 [50–79]	–		3T [1]	DTI	Connectivity maps for FA, FN & FL	BPANN (with GA & LM)	LOO	0.80	4.29	5.09	–	
Mwangi et al. (2013)[d]	188	[4–85]	–		3T [1]	DTI	FA	RVR (Gaussian RBF kernel)	LOO	0.87	8.20	10.60	–	
							MD			0.90	7.10	8.96		
							AD			0.89	7.16	9.19		
							RD			0.90	6.94	8.85		
Neeb et al. (2006)	44 [48%]	46 ± 15[k] [23–74]	–		1.5T [1]	T1, T2*	Quantitative water maps	LDA	LOO	0.69	6.30	–	–	
Sabuncu and Leemput (2011, 2012)[a,d]	336 [62%]	44 ± 24 [18–93]	–		1.5T [1]	T1	GM density (voxelwise)	Linear RVoxM	Half-split (2011)/5-fold CV (2012)	0.92 (2011)/ 0.94 (2012)	–	9.5 (2011)/ 7.9 (2012)	–	
								Linear RVM		0.90 (2011)/ 0.90 (2012)	–	10.2 (2011)/ 9.9 (2012)	–	
								RVoxM-NoReg		0.91 (2011)/ 0.93 (2012)	–	10.0 (2011)/ 8.9 (2012)	–	
Schnack et al. (2016)	386	34 ± 12 [16–67]	5	25–35	1.5T [1]/ 3T [1]	T1	GMV (voxelwise)	Linear SVR	LOO	0.89	4.31	–	–	3.86
Steffener et al. (2016)	331 [55%]	51 ± 18[k] [19–79]	–		3T [1]	T1	GMV (per ROI)	SSM	Bootstrap resampling	0.80	–	–	–	
Tian et al. (2016)[d]	63 [35%]	31 ± 9 [18–45]	–		3T [1]	rs-fMRI	resting-state functional connectivities	Elastic net (with LASSO)	LOO	0.78	4.81	–	–	

Table 3 (*continued*)

Study	Training sample (healthy subjects)		Independent test sample		MRI training [no of scanners]/ MRI test [no of scanners]	Modalities	Quantitative parameters used for brain age modeling	Algorithm for age modeling	Train-Test split for validation	Prediction performance in training sample			Prediction performance in test sample	
	No [female]	Age mean ± SD (yrs) [range]	No (female)	Age mean ± SD (yrs) [range]						r	MAE (yrs)	RMSE (yrs)	r	MAE (yrs)
Wang and Pham (2011)[d]	20	65 ± 10[k] [50–86]	–		1.5T [1]	T1	DWT from GM, WM & CSF (regionwise)	HMM	LOO	0.67[k]	6.20[k]	8.05[k]	–	
	11	64 ± 9[k] [51–76]								0.56[k]	6.18[k]	8.18[k]		
	8	62 ± 9[k] [52–76]								0.63[k]	8.00[k]	8.93[k]		
Wang et al. (2014)[d]	360 [51%]	47 ± 16 [20–82]	–		1.5T [2], 3T [1]	T1	Cortical thickness, mean curvature, Gaussian curvature, surface area (all regionwise)[j]	RVR (Gaussian kernel)	10-fold CV	0.93[i]	5.06[i]	6.10[i]	–	
							Cortical thickness, mean curvature, Gaussian curvature			0.94	4.57	5.57		
							Mean curvature, Gaussian curvature			0.82	7.47	9.18		
							Cortical thickness			0.89	6.05	7.37		
							Mean curvature			0.81	7.88	9.55		
							Gaussian curvature			0.55	11.21	13.64		
							Surface area			0.60	10.52	12.96		

– = data not given or not applicable; AD = axial diffusivity; BPANN = back propagation artificial neural network; CBR = correlationbasedregression; CV = cross-validation; DTI = diffusion tensor imaging; DWT = discrete wavelet transform; FA = fractional anisotropy; FL = fiber length; FLAIR = fluid-attenuated inversion recovery; FN = fiber number; GA = genetic algorithm; GMV = grey matter volume; GPR = Gaussian process regression; HC = healthy control; HMM = hidden Markov model; ICA = independent component analysis; kNNc = k-nearest neighbour clustering method; LASSO = least absolute shrinkage and selection operator; LM = Levenberg–Marquardt algorithm; LOO = leave-one-out; MAE = mean absolute error between brain age and chronological age; MD = mean diffusity; MO = mode of diffusion tensor; NAF = neighbourhood approximation forests; PLSR = partial least square regression; R2* = relaxation rate; RBF = radial basis function; RD = radial diffusivity; RMSE = root mean squared error; ROI = region of interest; rs-fMRI = resting-state functional MRI; RVM = relevance voxel machine; RVoxM = relevance voxel machine; RVoxM-NoReg = RVoxM without spatial regularization; RVR = relevance vector regression; SD = standard deviation; SSM = scaled subprofile modeling; SVR = support vector regression; WMV = white matter volume

(diff.) Test data were acquired on a different MRI scanner than training data.

^a This study compared different modeling methods.

^b The number denotes the width of the RBF kernel.

^c Results are given for modeling brain aging with concatenated GM & WM density maps resulting from small/large deformation algorithms.

^d Data from publicly available databases. For more details on the data please refer to the cited paper.

^e Results are given for modeling brain aging with/without applying principal component analysis (PCA) before generating the brain age model.

^f This study used data from healthy and cognitively diseased subjects to model and predict brain age.

^g The study provides training errors (LOO within the training sample) and test errors (for the left-out 1/3 of the whole study sample).

^h Results are given for modeling brain aging with NAF/kNNc algorithms.

ⁱ Performance for model including all modalities as input. Performance measures using modality subsets are given below.

^k Recalculated by the authors of the review paper.

et al., 2017). This approach showed a very good performance during cross-validation within the reference sample (combined model: r = 0.93, MAE = 4.3 years), but a rather fair generalizability when validating the brain age model in an independent sample of healthy subjects, with data acquired on a different scanner (combined model: r = 0.86, MAE = 8.0 years).

Three other studies used parameters derived from DTI as the only MRI modality (Han et al., 2014; Lin et al., 2016; Mwangi et al., 2013). Best prediction performances in the reference samples were obtained utilizing *relevance vector regression* (r = 0.90, MAE = 6.9 years; Mwangi et al., 2013) or an *artificial neural network approach* (r = 0.80, MAE = 4.3 years; Lin et al., 2016). Again, these studies neither validated their brain age models across scanners, nor in independent test samples.

Most of the studies generating models for brain aging during adulthood used parameters from T1-weighted MRI only, deriving voxel- or regionwise tissue volumes or cortical measures. Best prediction accuracies during cross-validation in the reference samples as well as during validation of the brain age model in independent test samples were achieved utilizing *relevance vector regression* (reference sample: r = 0.94, MAE = 4.6 years; independent test sample: r = 0.89, MAE = 5.4 years; Franke et al., 2010), *linear support vector regression* (reference sample: r = 0.89, MAE = 4.3 years; independent test sample: MAE = 3.9 years; Schnack et al., 2016), or *Gaussian process regression* (reference sample: r = 0.92, MAE = 6.2 years; independent test sample: r = 0.93, MAE = 5.8 years; Cole et al., 2015).

Depending on the choice of MRI modalities, derived parameters, mathematical approaches and numbers of subjects in the reference samples used for generating the brain age prediction model, and age ranges in the reference and independent test samples, diverging accuracies for brain age prediction have been reported. In general, prediction accuracy was improved in multimodal models including parameters derived from DTI. Although DTI is a powerful tool offering unique information on tissue microstructure and neural fiber connections that cannot be obtained from standard structural MRI, parameters derived from DTI can differ significantly depending on the type of scanner, field strength, gradient strength, number of gradient orientations, preprocessing, fitting procedure, tractography algorithm etc. (Jones and Cercignani, 2010; Jones et al., 2013; Tournier et al., 2011; Van Hecke et al., 2015). Unfortunately, all reviewed studies including DTI failed to prove generalizability of the established brain age model in independent test samples and across scanners.

4.5. Application of brain age biomarkers in healthy and diseased populations

Some of the brain age models described in this review have already been applied to neuropsychological and clinical questions. In multimodal models for structural brain development, advanced brain maturation was related to superior cognitive performances (Erus et al., 2015; Khundrakpam et al., 2015). Applying a brain maturation model based on voxelwise GM and WM volume, delayed brain maturation has been shown in adolescents born very preterm (Franke et al., 2012b). Established and validated models for brain aging showed significant relationships between individual brain ages and health and lifestyle variables, and medical drug use (Franke et al., 2014; Habes et al., 2016). Lower brain ages than chronological age were found to be associated with higher levels of education and physical activity (Steffener et al., 2016) as well as higher levels of meditation practice (Luders et al., 2016). Evidence of advanced brain aging has been provided for traumatic brain injury (Cole et al., 2015), epilepsy (Pardoe et al., 2017), HIV (Cole et al., 2017d), DS (Cole et al., 2017a), diabetes (Franke et al., 2013), schizophrenia (Koutsouleris et al., 2014; Schnack et al., 2016), MCI and AD (Franke et al., 2012a; Franke et al., 2010; Gaser et al., 2013), and in elderly people who had previously suffered undernutrition during gestation (Franke et al., 2017a, 2017b). Furthermore,

advanced brain aging was shown to be indicative of poorer physical fitness, lower fluid intelligence, higher allostatic load, and increased mortality (Cole et al., 2017c), and even predictive of the onset of cognitive decline (Franke et al., 2012a; Gaser et al., 2013).

5. A biomarker for cognitive brain development and aging

5.1. Cognitive information processing capacity across the lifespan

The famous quote of Mortimer Mishkin, "[brain] imaging is not enough", is still valid. Therefore, structural imaging data have to be accompanied by an assessment of cognition to estimate the functional consequences of brain lesions. Cognition is typically considered and assessed as a multifaceted concept comprising a variety of different capabilities (Kanwisher, 2010). It is also well established that different abilities share a substantial commonality: A subject who acts smartly on task A tends to perform efficiently also on task B, even if both tasks belong to different cognitive domains, such as language and visuospatial functions. Such concordance is assumed to result from a general cognitive aptitude, or a "g-factor" of intelligence, that subserves all aspects of intellectual functioning (Spearman, 1904) and has been associated with a multiple-demand brain system involving the fronto-parietal cortex (Duncan, 2013). This general factor is especially involved in non-routine tasks requiring novel problem solving, which are commonly known as tests of "fluid intelligence". The level of intelligence, i.e. the relative position of an individual within his/her age cohort, remains strikingly stable across the lifespan (Deary et al., 2013). Inter-individual differences are attributed to variations of brain connectivity and physiology (Jung and Haier, 2007), which determine the efficiency of basic information processing at the core of the cognitive 'mechanics' (Baltes et al., 1999).

Two important lifespan determinants of cognitive mechanics have been identified, i.e., the information-processing rate and the short-term storage of information. They build an individual's cognitive processing capacity and point to basic constraints for cognitive efficiency: the amount of information that can be maintained in parallel in an active state; and the speed with which active representations can be accessed for further processing (Barrouillet and Camos, 2012). These aspects undergo considerable change across the lifespan with a relatively steep increase during childhood development and early adulthood, followed by a gradual decline with increasing age (Baltes et al., 1999). If it would be possible to validly assess the basic mechanics of cognition, such a method could serve as a valuable tool providing information on the efficiency of cognitive performance on a larger scale and serving as an appropriate marker for functional brain development and aging. As the cerebral system underlying visual attention permeates the scaffolding of cognition at all hierarchical levels of the brain (Petersen and Posner, 2012), including the fronto-parietal cortex (Ptak, 2012), the analysis of visual perceptual speed and visual short-term memory storage is a candidate approach to serve this purpose.

5.2. Efficiency of visual information uptake as a marker of cognitive development and aging

Extracting information from brief visual displays is a cognitive ability that reflects fundamental capacity limitations of human information processing (Luck and Vogel, 2013) and relates to fluid intelligence (Deary, 2001). It also undergoes significant decline during aging, as has been shown with a number of different assessment procedures. The "useful field of view" (UFOV) task, for example, provides a measure of visual processing speed (Wood and Owsley, 2014). More specifically, it assesses the presentation time at which stimuli can be detected at 75% accuracy under varying conditions of saliency. The speed estimate has been shown to be associated in the elderly with a range of functional outcomes of daily living, among them driving ability, crash risk, mobility, balance control, and risk of falling.

Measurable improvement has also been revealed during middle to late childhood (Bennett et al., 2009).

Another method, the "inspection time" (IT) task, is a two-alternative forced choice and backward masking test involving a simple visual discrimination between two lines of markedly different lengths (Deary, 2001). By assessing performance accuracy as a function of presentation time in this task, an estimation of the speed of visual information uptake is derived. This speed measure has been shown to decline with age, with the decline being strongly associated with a decrease of the intelligence level (Ritchie et al., 2014). Variants of this task have also been applied to children as young as 4 years of age (Williams et al., 2009).

The results acquired with these tasks are in line with the processing speed account of cognitive ageing. This account maintains that the age-related decline in higher cognitive functions results from a reduced efficiency with which simple mental operations can be completed (Salthouse, 1996). In contrast to response time or psychomotor tasks such as digit symbol substitution, UFOV and IT more purely reflect mental speed, because they do not contain motor aspects. However, even in the extraction of briefly presented stimuli, separable components of information uptake are involved that cannot be differentiated by these tasks (Espeseth et al., 2014). A disentanglement of these components is accomplished by the 'theory of visual attention'.

5.3. The 'theory of visual attention' (TVA) as a framework for modeling the efficiency of visual information uptake

The 'theory of visual attention' (TVA) was first proposed by Bundesen (1990) and has since then advanced systematically (Bundesen and Habekost, 2008; Bundesen et al., 2015). TVA is a computational model of visual selective attention with a strong association to the biased-competition framework (Desimone and Duncan, 1995). It accounts for a broad range of data from "attention" literature, derived both from behavioral studies in human subjects and from single-cell recordings in the monkey (Bundesen et al., 2005).

In short, TVA assumes that the visual processing system accumulates evidence on objects in the environment until enough information is sampled to decide on an object's identity (i.e. recognition is possible). This process is more or less an oscillatory interaction between long-term memory representations and the perceptual features available from the environment (Kyllingsbaek, 2006). During this process, an unselective stage of massive parallel matching between memory representations (within the visual association cortex) and environmental input is funneled into a selective stage. Here (purportedly by way of cortico-subcortical and, in particular, thalamo-cortical interactions), allocation of attentional capacity is biased towards those visual events, which have gained higher evidence for their "objectness".

A representative scenario of this process is realized by a simple psychophysical task involving a flash presentation of letter arrays. In one variant of this task, "whole report", letters are briefly presented in a circular arrangement with an individually adjusted presentation time and are either masked or unmasked. The subjects' task is to report as many letters as possible (Fig. 4). Based on the basic equations provided by TVA (see Bundesen, 1990; Bundesen and Habekost, 2008; Kyllingsbaek, 2006), the probability of a correct letter report as a function of effective exposure duration is modeled for each subject by an exponential growth function. Fitting this function according to a maximum likelihood method is undertaken by estimating four parameters, which determine the shape of the curve (Fig. 5). Shape variations resulting from different parameter values represent individual differences of visual processing capacity.

The three important parameter values provided by TVA are: (1) parameter t_0 (expressed in milliseconds), the estimated threshold value (minimum presentation time) beneath which nothing is perceived (i.e. probability of report equals 0); (2) parameter C, an estimation of visual processing speed (rate of information uptake, expressed in numbers of
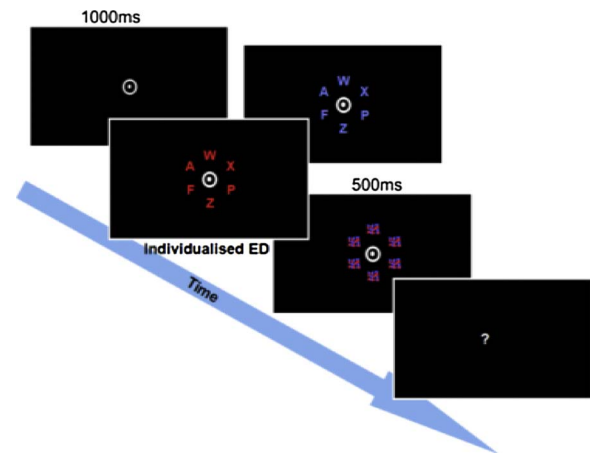

Fig. 4. Typical trial of a whole report task. Six circularly arranged letters are briefly flashed on a computer screen with variable exposure times (ED; e.g. 10–300 ms). The letters are either presented unmasked or followed by a mask that limits visual stimulus processing time to the duration of its physical availability. Subjects' task is to report as many letters as possible but refrain from guessing. Stimulus presentation time is individually adjusted to compensate for differences in baseline performance.

elements processed per second), which reflects the slope of the exponential growth function at its origin at the coordinate (t_0, 0); and (3) parameter K, an estimation of visual short-term memory (VSTM) storage capacity (the maximum number of objects that can be represented simultaneously at a given time in VSTM, expressed in number of elements), reflecting the asymptote of the exponential growth function. The reliability of these parameter estimates can be derived at the level of each individual subject by a bootstrapping procedure (Kyllingsbaek, 2006).

Hitherto, assessment of the life-span development and age-related change of TVA-based parameter estimates (Espeseth et al., 2014; Habekost et al., 2013; McAvinue et al., 2012; Wilms and Nielsen, 2014) has collectively involved far more than 400 subjects with ages ranging from 12 to 87 years. As summarized by Habekost (2015), cognitive aging according to TVA is characterized by an increase of the perceptual threshold and a decrease of processing speed and VSTM storage capacity. These modifications might reflect loss of whole brain volume due to the decrease of grey and white matter that is associated with normal aging (Good et al., 2001; Knoops et al., 2012). After all, in a TVA-based study in normal subjects, Chechlacz et al. (2015) found that individual differences in K and C parameter values are directly linked to structural differences within the long-association fronto-parietal white matter. And Bublak et al. (2011), in their study on early AD observed an increase of the perceptual threshold at the MCI stage where a primary cortical pathology can be assumed. In contrast, a decline of VSTM storage capacity and processing rate was observed only at the dementia stage, when white matter connectivity is additionally affected. Taken together, these data strongly suggest the suitability of TVA-derived parameter estimates − either separately or in combination − as markers of cognitive aging and as predictors of age-related neurodegenerative diseases. However, the accuracy and the relationship of TVA-derived parameter estimates with parameters such as brain age still remain to be established. To date, the approach has been successfully applied to a range of neurological and psychiatric conditions (for review see Habekost, 2015) where it has proven to be a promising tool especially for analyzing cognitive performance in diffusely disseminated brain disorders.

6. Summary

Until recently, inferences from research data in the fields of biomedical and neurosciences were mainly based on classical statistical methods such as null-hypothesis testing operating at the group-level.
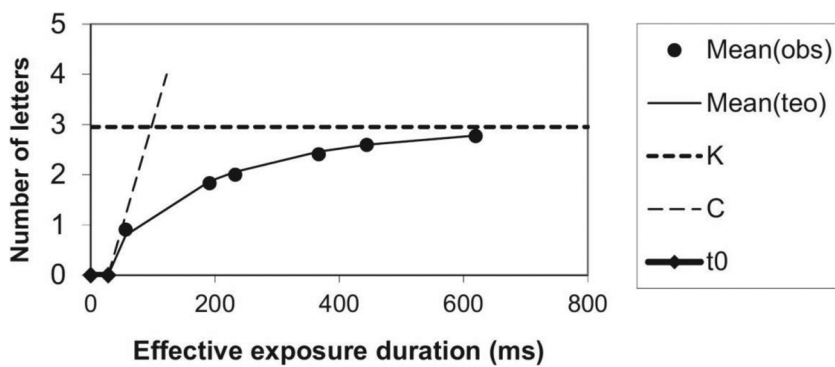
Fig. 5. Fitting performance in the whole report task. Black dots represent the mean number of letters correctly reported by a subject (Mean(obs)), as a function of stimulus duration. The solid curve represents the maximum likelihood fit to these observations (Mean (teo)), as derived from TVA. Three parameters estimated by TVA are shown: perceptual threshold (t_0 = origin of the curve at the abscissa), visual processing speed (C = slope of the curve at its origin), and visual short-term memory storage capacity (K = the curve's asymptote).

Now, data-driven learning methods, including cross-validation, pattern classification, and regression-based predictive analyses, exemplify a new trend that allow measurements and predictions even at the single subject level (Bzdok, 2016).

Herein, we reviewed and discussed studies, which investigated cellular, structural and functional biomarkers of brain development and aging using different methods and across age ranges from the fetal stage to older age. We determined that a number of attempts have been made to develop personalized biomarkers for assessing biological brain aging. At the cellular and more mechanistic level, TL as well as the epigenetic clock appear to be promising because it fulfills basic requirements for a marker of aging according to the American Federation of Aging Research (Sprott, 2010). According to these guidelines, the markers should possess certain characteristics. For example, they should be able to determine biological aging, predict the rate of aging, monitor a fundamental process that underlies aging, and be measured accurately, efficiently, and repeatedly without harming the subject. Further, the markers need to be applicable across the species. Indeed, peripheral TL as well as epigenetic clock measurements are readily available in humans. TL and the epigenetic clock measurements are reliable and efficient, although sensitivity and accuracy varies widely across labs and methods used. Thus TL and epigenetic clocks are actually not suitable for multi-center studies or for performing comparisons between studies or even between subjects. Consequently, the potential of TL and epigenetic clocks in determining general biological or brain age is currently far away from a direct clinical application. Although a number of studies available in the literature suggest that peripheral TL and epigenetic clock measurements might indeed be a useful future biomarker of biological age at least in older populations, they do not appear to represent a general biomarker or, more specifically, a brain-specific of aging since they are not solely associated to aging and age-related diseases. If LTL and epigenetic clocks were truly associated with a general phenotype, one would ideally observe consistency across populations, measurement methods, and statistical models. But to date, TL and epigenetic clocks are considered a weak marker with poor deterministic and predictive accuracy (as thoroughly discussed in chapter 2). Bearing in mind all those issues discussed above, it is unlikely that TL and epigenetic clock measurements could be used as a single biomarker for brain aging in near future.

Although biomarkers of aging were called for to be preferably be closely related to the mechanistic aging process, development of markers of brain aging, which are related to brain function and structure, is much more advanced and provide a considerably higher degree of correlation to age and diagnostic specificity. Moreover, these markers show less inter-individual variability as well as methodological variations of measurements across labs or study sites. The superiority of phenotype-related markers may be explained on a number of grounds: At present it is easier to determine phenotype because the processes underlying brain aging are complex and not yet well understood. Moreover, the organism modulates and responds to the process of aging in the biological environment through a large variety of compensatory pathways. In contrast to the complexity of pathways at the cellular level, the organism can respond to an infinite number of biological and environmental influences with only limited changes to the phenotype. Consequently, phenotype-related biomarkers based on functional and structural brain development and aging probably better reflect and longitudinally track individual brain aging trajectories.

Potentially promising phenotype-related biomarkers of functional brain aging are those markers that measure cognitive function – if possible at a global level. Cognitive function is closely related to age during development and aging (Baltes et al., 1999). Age-related cognitive decline is a major and growing concern in many modern societies since mental health is perceived as a major determinant limiting quality of life during aging (Puvill et al., 2016). Thus, biomarkers measuring individual cognitive brain age and predicting individual trajectory of cognitive decline are highly desirable. Studies in childhood or adulthood that were based on cognitive information processing capacity as a global biomarker for brain function demonstrated the potential of capturing individual trajectories of cognitive brain aging, detecting alterations in neurological and psychiatric conditions, and even predicting age-related neurodegenerative diseases. Of course, at present, this is a promise that has to be filled by further studies demonstrating the accuracy of functional age estimation, its relation to brain age, as well as to measures of intellectual ability. The occurrence of neuropsychiatric and neurodegenerative diseases and the trajectories of cognitive and functional brain aging are most likely, at least partly, determined *in utero* (Gluckman et al., 2008; Tarry-Adkins and Ozanne, 2014; Van den Bergh, 2011). Consequently, first attempts have been made to detect aberrations of functional fetal brain development as a prerequisite for early preventive or interventional measures. Determination of the activity of the ANS by HRV analysis is a clinically promising approach to detect the stage of fetal functional brain development. The activity of fetal ANS regulated by central nervous control mechanisms is quite easily accessible via analysis of fetal HRP. A functional fetal autonomic brain age score has been developed which estimates fetal functional brain age with an accuracy of 3 wG from about 15 wG onwards in 30 min fMCG recordings. It was validated across fMCG study centers with loss of precision in shorter (5 min) recordings and across recording technologies with loss of precision in CTG recordings (Hoyer et al., 2015; Hoyer et al., 2017). It provides a comprehensive marker of fetal functional brain development and its disturbances.

Approaches to determine brain age based on structural neuroimaging data are designed to indicate deviations in age-related spatiotemporal brain changes by establishing reliable reference curves for healthy brain aging and providing individual brain age measures, while accounting for the multidimensional aging patterns across the brain. In volumetric studies, "healthy" brain aging has been found to follow highly coordinated and sequenced patterns of brain tissue loss and CSF expansion on a general and rather superficial level (Raz and Rodrigue, 2006; Resnick et al., 2003; Terribilli et al., 2011), thus allowing for a robust modeling of "healthy" brain aging via modern pattern

recognition techniques. On the other hand, multiple factors are suggested to and have already been shown to affect and modify individual brain aging trajectories, thus stressing the need and usefulness of those modern MRI-based biomarkers for individual brain aging. Reliability studies for MRI-based brain aging biomarkers showed high test-retest performance at the same scanner as well as between scanners, with intraclass correlation coefficients (ICC) of 0.93 and 0.90, respectively (Franke et al., 2012a) and ICC of 0.96–0.98 and 0.77–0.96, respectively (Cole et al., 2017b). Furthermore, several studies applying the MRI-based models for structural brain aging, have already demonstrated profound relationships between premature brain aging and AD disease severity and prospective worsening of cognitive functions (Franke et al., 2012a), MCI and AD (Ziegler et al., 2014), conversion to AD (Gaser et al., 2013), schizophrenia (Koutsouleris et al., 2014; Schnack et al., 2016), traumatic brain injury (Cole et al., 2015), HIV (Cole et al., 2017d), diabetes mellitus type 2 (Franke et al., 2013), and elderly people suffering from undernutrition during gestation (Franke et al., 2017a, 2017b), as well as being indicative of poorer physical fitness, lower fluid intelligence, higher allostatic load, and increased mortality (Cole et al., 2017c). Additionally, significant associations between individual brain aging and several health- and lifestyle-related risk factors and drug use in the general population (Franke et al., 2014; Habes et al., 2016), levels of education and physical activity (Steffener et al., 2016) and meditation practice (Luders et al., 2016) have been shown.

In conclusion, the phenotypic approaches presented here have already established and validated reference curves for age-related changes in brain structure and function. Furthermore, they also showed great potential for easy application in multi-center studies. Thus, these predictive analytical methods provide individualized biomarkers for determining the biological age of brain structure and function. The MRI- and cerebral processing capacity-based markers are able to predict individual aberrations in brain development and aging as well as the occurrence of age-related cognitive decline and age-related neurodegenerative diseases. This review has gathered evidence that neuroimaging data and fetal HRP as well as cognitive data can be used to establish biomarkers for brain aging, which have already been confirmed as providing vital prognostic information. In future, combining different biomarkers of structural and functional brain age may enhance sensitivity and specificity for detecting aberrations in biological age compared to the chronological age in various neurological and psychiatric conditions and in neurodegenerative diseases. The important prognostic information included in the estimation of the structural and functional brain age may aid in developing personalized neuroprotective treatments and interventions.

Acknowledgements

References

Ahlbom, E., Gogvadze, V., Chen, M., Celsi, G., Ceccatelli, S., 2000. Prenatal exposure to high levels of glucocorticoids increases the susceptibility of cerebellar granule cells to oxidative stress-induced cell death. Proc. Natl. Acad. Sci. U. S. A. 97, 14726–14730.

Antonelli, M.C., Pallares, M.E., Ceccatelli, S., Spulber, S., 2017. Long-term consequences of prenatal stress and neurotoxicants exposure on neurodevelopment. Prog. Neurobiol. 155, 21–35.

Antonow-Schlorke, I., Schwab, M., Li, C., Nathanielsz, P.W., 2003. Glucocorticoid exposure at the dose used clinically alters cytoskeletal proteins and presynaptic terminals in the fetal baboon brain. J. Physiol. 547, 117–123.

Arbabshirani, M.R., Plis, S., Sui, J., Calhoun, V.D., 2017. Single subject prediction of brain disorders in neuroimaging: promises and pitfalls. Neuroimage 145, 137–165.

Ashburner, J., 2007. A fast diffeomorphic image registration algorithm. Neuroimage 38, 95–113.

Aviv, A., 2012. Genetics of leukocyte telomere length and its role in atherosclerosis. Mutat. Res. 730, 68–74.

Baird, F.J., Bennett, C.L., 2013. Microtubule defects & neurodegeneration. J. Genet. Syndr. Gene Ther. 4, 203.

Bakaysa, S.L., Mucci, L.A., Slagboom, P.E., Boomsma, D.I., McClearn, G.E., Johansson, B., Pedersen, N.L., 2007. Telomere length predicts survival independent of genetic influences. Aging Cell 6, 769–774.

Baker 3rd, G.T., Sprott, R.L., 1988. Biomarkers of aging. Exp. Gerontol. 23, 223–239.

Bale, T.L., 2015. Epigenetic and transgenerational reprogramming of brain development. Nat. Rev. Neurosci. 16, 332–344.

Baltes, P.B., Staudinger, U.M., Lindenberger, U., 1999. Lifespan psychology: theory and application to intellectual functioning. Annu. Rev. Psychol. 50, 471–507.

Barker, D.J., 1998. In utero programming of chronic disease. Clin. Sci. 95, 115–128.

Barrett, E.L., Richardson, D.S., 2011. Sex differences in telomeres and lifespan. Aging Cell 10, 913–921.

Barrouillet, P., Camos, V., 2012. As time goes by. Curr. Direct. Psychol. Sci. 21, 413–419.

Belnoue, L., Grosjean, N., Ladeveze, E., Abrous, D.N., Koehl, M., 2013. Prenatal stress inhibits hippocampal neurogenesis but spares olfactory bulb neurogenesis. PLoS One 8, e72972.

Belsky, D.W., Moffitt, T.E., Cohen, A.A., Corcoran, D.L., Levine, M.E., Prinz, J., et al., 2016. Telomere, epigenetic clock, and biomarker-composite quantifications of biological aging: do they measure the same thing? bioRxiv.

Bennett, D.M., Gordon, G., Dutton, G.N., 2009. The useful field of view test, normative data in children of school age. Optom. Vis. Sci. 86, 717–721.

Bertalanffy, L.v., 1968. General System Theory: Foundations, Development, Applications. Braziller, New York, NY.

Bhatia-Dey, N., Kanherkar, R.R., Stair, S.E., Makarev, E.O., Csoka, A.B., 2016. Cellular senescence as the causal nexus of aging. Front. Genet. 7, 13.

Biegler, K.A., Anderson, A.K., Wenzel, L.B., Osann, K., Nelson, E.L., 2012. Longitudinal change in telomere length and the chronic stress response in a randomized pilot biobehavioral clinical study: implications for cancer prevention. Cancer Prev. Res. (Phila) 5, 1173–1182.

Blackburn, E.H., Greider, C.W., Szostak, J.W., 2006. Telomeres and telomerase: the path from maize, Tetrahymena and yeast to human cancer and aging. Nat. Med. 12, 1133–1138.

Blackburn, E.H., 2000. Telomere states and cell fates. Nature 408, 53–56.

Blaze, J., Asok, A., Roth, T.L., 2015. The long-term impact of adverse caregiving environments on epigenetic modifications and telomeres. Front. Behav. Neurosci. 9, 79.

Boccardi, V., Pelini, L., Ercolani, S., Ruggiero, C., Mecocci, P., 2015. From cellular senescence to Alzheimer's disease: the role of telomere shortening. Ageing Res. Rev. 22, 1–8.

Bocklandt, S., Lin, W., Sehl, M.E., Sanchez, F.J., Sinsheimer, J.S., Horvath, S., Vilain, E., 2011. Epigenetic predictor of age. PLoS One 6, e14821.

Breitling, L.P., Saum, K.U., Perna, L., Schottker, B., Holleczek, B., Brenner, H., 2016. Frailty is associated with the epigenetic clock but not with telomere length in a German cohort. Clin. Epigenet. 8, 21.

Broer, L., Codd, V., Nyholt, D.R., Deelen, J., Mangino, M., Willemsen, G., et al., 2013. Meta-analysis of telomere length in 19, 713 subjects reveals high heritability, stronger maternal inheritance and a paternal age effect. Eur. J. Hum. Genet. 21, 1163–1168.

Brown, T.T., Kuperman, J.M., Chung, Y., Erhart, M., McCabe, C., Hagler Jr., D.J., et al., 2012. Neuroanatomical assessment of biological maturity. Curr. Biol. 22, 1693–1698.

Bublak, P., Redel, P., Sorg, C., Kurz, A., Forstl, H., Muller, H.J., et al., 2011. Staged decline of visual processing capacity in mild cognitive impairment and Alzheimer's disease. Neurobiol. Aging 32, 1219–1230.

Bundesen, C., Habekost, T., 2008. Principles of Visual Attention: Linking Mind and Brain. Oxford University Press, Oxford; New York.

Bundesen, C., Habekost, T., Kyllingsbaek, S., 2005. A neural theory of visual attention: bridging cognition and neurophysiology. Psychol. Rev. 112, 291–328.

Bundesen, C., Vangkilde, S., Petersen, A., 2015. Recent developments in a computational theory of visual attention (TVA). Vision Res. 116, 210–218.

Bundesen, C., 1990. A theory of visual attention. Psychol. Rev. 97, 523–547.

Buss, C., Davis, E.P., Shahbaba, B., Pruessner, J.C., Head, K., Sandman, C.A., 2012. Maternal cortisol over the course of pregnancy and subsequent child amygdala and hippocampus volumes and affective problems. Proc. Natl. Acad. Sci. U. S. A. 109, E1312–1319.

Bzdok, D., 2016. Classical Statistics and Statistical Learning in Imaging Neuroscience. arXiv:1603.01857.

Cai, Z., Yan, L.J., Ratka, A., 2013. Telomere shortening and Alzheimer's disease. Neuromol. Med. 15, 25–48.

Campisi, J., d'Adda di Fagagna, F., 2007. Cellular senescence: when bad things happen to good cells. Nat. Rev. Mol. Cell Biol. 8, 729–740.

Cao, B., Mwangi, B., Hasan, K.M., Selvaraj, S., Zeni, C.P., Zunta-Soares, G.B., Soares, J.C., 2015. Development and validation of a brain maturation index using longitudinal neuroanatomical scans. Neuroimage 117, 311–318.

Cao-Lei, L., de Rooij, S., King, S., Matthews, S., Metz, G., Roseboom, T., Syzf, M., 2017. Prenatal stress and epigenetics. Neurosci. Biobehav. Rev this issue.

Charil, A., Laplante, D.P., Vaillancourt, C., King, S., 2010. Prenatal stress and brain development. Brain Res. Rev. 65, 56–79.

Chechlacz, M., Gillebert, C.R., Vangkilde, S.A., Petersen, A., Humphreys, G.W., 2015. Structural variability within frontoparietal networks and individual differences in attentional functions: an approach using the theory of visual attention. J. Neurosci. 35, 10647–10658.

Chen, W., Kimura, M., Kim, S., Cao, X., Srinivasan, S.R., Berenson, G.S., et al., 2011. Longitudinal versus cross-sectional evaluations of leukocyte telomere length

dynamics: age-dependent telomere shortening is the rule. J. Gerontol. A. Biol. Sci. Med. Sci. 66, 312–319.

Chen, B.H., Marioni, R.E., Colicino, E., Peters, M.J., Ward-Caviness, C.K., Tsai, P.C., et al., 2016. DNA methylation-based measures of biological age: meta-analysis predicting time to death. Aging (Albany NY) 8, 1844–1865.

Cherubini, A., Caligiuri, M.E., Peran, P., Sabatini, U., Cosentino, C., Amato, F., 2016. Importance of multimodal MRI in characterizing brain tissue and its potential application for individual age prediction. IEEE J. Biomed. Health Inform. 20, 1232–1239.

Christensen, K., McGue, M., Petersen, I., Jeune, B., Vaupel, J.W., 2008. Exceptional longevity does not result in excessive levels of disability. Proc. Natl. Acad. Sci. U. S. A. 105, 13274–13279.

Cohen, J.R., Asarnow, R.F., Sabb, F.W., Bilder, R.M., Bookheimer, S.Y., Knowlton, B.J., Poldrack, R.A., 2011. Decoding continuous variables from neuroimaging data: basic and clinical applications. Front. Neurosci. 5, 75.

Cole, J.H., Franke, K., 2017. Predicting age using neuroimaging: a brain ageing biomarker. Trends Neurosci. 40, 1.

Cole, J.H., Leech, R., Sharp, D.J., DiseaseAlzheimer's Disease Neuroimaging, I., 2015. Prediction of brain age suggests accelerated atrophy after traumatic brain injury. Ann. Neurol. 77, 571–581.

Cole, J.H., Annus, T., Wilson, L.R., Remtulla, R., Hong, Y.T., Fryer, T.D., et al., 2017a. Brain-predicted age in Down syndrome is associated with beta amyloid deposition and cognitive decline. Neurobiol. Aging 56, 41–49.

Cole, J.H., Poudel, R.P.K., Tsagkrasoulis, D., Caan, M.W.A., Steves, C., Spector, T.D., Montana, G., 2017b. Predicting brain age with deep learning from raw imaging data results in a reliable and heritable biomarker. Neuroimage 163, 115–124.

Cole, J.H., Ritchie, S.J., Bastin, M.E., Valdes Hernandez, M.C., Munoz Maniega, S., Royle, N., et al., 2017c. Brain age predicts mortality. Mol. Psychiatry in press.

Cole, J.H., Underwood, J., Caan, M.W., De Francesco, D., van Zoest, R.A., Leech, R., et al., 2017d. Increased brain-predicted aging in treated HIV disease. Neurology 88, 1349–1357.

Colpo, G.D., Leffa, D.D., Kohler, C.A., Kapczinski, F., Quevedo, J., Carvalho, A.F., 2015. Is bipolar disorder associated with accelerating aging? A meta-analysis of telomere length studies. J. Affect. Disord. 186, 241–248.

D'Mello, M.J., Ross, S.A., Briel, M., Anand, S.S., Gerstein, H., Pare, G., 2015. Association between shortened leukocyte telomere length and cardiometabolic outcomes: systematic review and meta-analysis. Circ. Cardiovasc. Genet. 8, 82–90.

David, M., Hirsch, M., Karin, J., Toledo, E., Akselrod, S., 2007. An estimate of fetal autonomic state by time-frequency analysis of fetal heart rate variability. J. Appl. Physiol. 102, 1057–1064.

Davis, E.P., Sandman, C.A., Buss, C., Wing, D.A., Head, K., 2013. Fetal glucocorticoid exposure is associated with preadolescent brain development. Biol. Psychiatry 74, 647–655.

de Rooij, S.R., Wouters, H., Yonker, J.E., Painter, R.C., Roseboom, T.J., 2010. Prenatal undernutrition and cognitive function in late adulthood. Proc. Natl. Acad. Sci. U. S. A. 107, 16881–16886.

Deary, I.J., Pattie, A., Starr, J.M., 2013. The stability of intelligence from age 11 to age 90 years: the Lothian birth cohort of 1921. Psychol. Sci. 24, 2361–2368.

Deary, I.J., 2001. Human intelligence differences: towards a combined experimental-differential approach. Trends Cogn. Sci. 5, 164–170.

Debnath, M., Venkatasubramanian, G., Berk, M., 2015. Fetal programming of schizophrenia: select mechanisms. Neurosci. Biobehav. Rev. 49, 90–104.

Deelen, J., Beekman, M., Codd, V., Trompet, S., Broer, L., Hagg, S., et al., 2014. Leukocyte telomere length associates with prospective mortality independent of immune-related parameters and known genetic markers. Int. J. Epidemiol. 43, 878–886.

Desimone, R., Duncan, J., 1995. Neural mechanisms of selective visual attention. Annu. Rev. Neurosci. 18, 193–222.

Desplats, P.A., 2015. Perinatal programming of neurodevelopment: epigenetic mechanisms and the prenatal shaping of the brain. Adv. Neurobiol. 10, 335–361.

DiPietro, J.A., Hodgson, D.M., Costigan, K.A., Hilton, S.C., Johnson, T.R., 1996. Fetal neurobehavioral development. Child Dev. 67, 2553–2567.

Dlouha, D., Maluskova, J., Kralova Lesna, I., Lanska, V., Hubacek, J.A., 2014. Comparison of the relative telomere length measured in leukocytes and eleven different human tissues. Physiol. Res. 63 (Suppl. 3), S343–S350.

Dodic, M., Hantzis, V., Duncan, J., Rees, S., Koukoulas, I., Johnson, K., et al., 2002. Programming effects of short prenatal exposure to cortisol. FASEB J. 16, 1017–1026.

Dosenbach, N.U., Nardos, B., Cohen, A.L., Fair, D.A., Power, J.D., Church, J.A., et al., 2010. Prediction of individual brain maturity using fMRI. Science 329, 1358–1361.

Duncan, J., 2013. The structure of cognition: attentional episodes in mind and brain. Neuron 80, 35–50.

Eisenberg, D.T., Tackney, J., Cawthon, R.M., Cloutier, C.T., Hawkes, K., 2017. Paternal and grandpaternal ages at conception and descendant telomere lengths in chimpanzees and humans. Am. J. Phys. Anthropol. 162, 201–207.

Eisenberg, D.T., 2011. An evolutionary review of human telomere biology: the thrifty telomere hypothesis and notes on potential adaptive paternal effects. Am. J. Hum. Biol. 23, 149–167.

Eitan, E., Hutchison, E.R., Mattson, M.P., 2014. Telomere shortening in neurological disorders: an abundance of unanswered questions. Trends Neurosci. 37, 256–263.

Electrophysiology, T.F.o.t.E.S.o.C.a.t.N.A.S.o.P.a., 1996. Heart rate variability: standards of measurement, physiological interpretation and clinical use. Task Force of the European Society of Cardiology and the North American Society of Pacing and Electrophysiology. Circulation 93, 1043–1065.

Entringer, S., Epel, E.S., Kumsta, R., Lin, J., Hellhammer, D.H., Blackburn, E.H., et al., 2011. Stress exposure in intrauterine life is associated with shorter telomere length in young adulthood. Proc. Natl. Acad. Sci. U. S. A. 108, E513–518.

Entringer, S., Buss, C., Wadhwa, P.D., 2012. Prenatal stress, telomere biology, and fetal

programming of health and disease risk. Sci. Signal. 5, pt12.

Entringer, S., Epel, E.S., Lin, J., Buss, C., Shahbaba, B., Blackburn, E.H., et al., 2013. Maternal psychosocial stress during pregnancy is associated with newborn leukocyte telomere length. Am. J. Obstet. Gynecol. 208 (134), e131–137.

Epel, E.S., Blackburn, E.H., Lin, J., Dhabhar, F.S., Adler, N.E., Morrow, J.D., Cawthon, R.M., 2004. Accelerated telomere shortening in response to life stress. Proc. Natl. Acad. Sci. U. S. A. 101, 17312–17315.

Erus, G., Battapady, H., Satterthwaite, T.D., Hakonarson, H., Gur, R.E., Davatzikos, C., Gur, R.C., 2015. Imaging patterns of brain development and their relationship to cognition. Cereb. Cortex 25, 1676–1684.

Espeseth, T., Vangkilde, S.A., Petersen, A., Dyrholm, M., Westlye, L.T., 2014. TVA-based assessment of attentional capacities-associations with age and indices of brain white matter microstructure. Front. Psychol. 5, 1177.

Faa, G., Marcialis, M.A., Ravarino, A., Piras, M., Pintus, M.C., Fanos, V., 2014. Fetal programming of the human brain: is there a link with insurgence of neurodegenerative disorders in adulthood? Curr. Med. Chem. 21, 3854–3876.

Favaro, A., Tenconi, E., Degortes, D., Manara, R., Santonastaso, P., 2015. Neural correlates of prenatal stress in young women. Psychol. Med. 45, 2533–2543.

Ferrario, M., Signorini, M.G., Magenes, G., 2009. Complexity analysis of the fetal heart rate variability: early identification of severe intrauterine growth-restricted fetuses. Med. Biol. Eng. Comput. 47, 911–919.

Ferron, S.R., Marques-Torrejon, M.A., Mira, H., Flores, I., Taylor, K., Blasco, M.A., Farinas, I., 2009. Telomere shortening in neural stem cells disrupts neuronal differentiation and neuritogenesis. J. Neurosci. 29, 14394–14407.

Forero, D.A., Gonzalez-Giraldo, Y., Lopez-Quintero, C., Castro-Vega, L.J., Barreto, G.E., Perry, G., 2016a. Meta-analysis of telomere length in Alzheimer's disease. J. Gerontol. A Biol. Sci. Med. Sci. 71, 1069–1073.

Forero, D.A., Gonzalez-Giraldo, Y., Lopez-Quintero, C., Castro-Vega, L.J., Barreto, G.E., Perry, G., 2016b. Telomere length in Parkinson's disease: a meta-analysis. Exp. Gerontol. 75, 53–55.

Franco, S., Blasco, M.A., Siedlak, S.L., Harris, P.L., Moreira, P.I., Perry, G., Smith, M.A., 2006. Telomeres and telomerase in Alzheimer's disease: epiphenomena or a new focus for therapeutic strategy? Alzheimers Dement. 2, 164–168.

Franke, K., Ziegler, G., Kloppel, S., Gaser, C., Disease, Alzheimer's, Neuroimaging, I., 2010. Estimating the age of healthy subjects from T1-weighted MRI scans using kernel methods: exploring the influence of various parameters. Neuroimage 50, 883–892.

Franke, K., Gaser, C., for the Alzheimer's Disease Neuroimaging Initiative, 2012a. Longitudinal changes in individual BrainAGE in healthy aging, mild cognitive impairment, and Alzheimer's disease. GeroPsych: J. Gerontopsychol. Geriatric Psychiatry 25, 235–245.

Franke, K., Luders, E., May, A., Wilke, M., Gaser, C., 2012b. Brain maturation: predicting individual BrainAGE in children and adolescents using structural MRI. Neuroimage 63, 1305–1312.

Franke, K., Gaser, C., Manor, B., Novak, V., 2013. Advanced *BrainAGE* in older adults with type 2 diabetes mellitus. Front. Aging Neurosci. 5, 90.

Franke, K., Ristow, M., Gaser, C., Alzheimer's Disease Neuroimaging, I., 2014. Gender-specific impact of personal health parameters on individual brain aging in cognitively unimpaired elderly subjects. Front. Aging Neurosci. 6, 94.

Franke, K., Gaser, C., de Rooij, S.R., Schwab, M., Roseboom, T.J., 2017a. Premature brain aging in humans exposed to maternal nutrient restriction during early gestation. NeuroImage. http://dx.doi.org/10.1016/j.neuroimage.2017.10.047.

Franke, K., van den Bergh, B., de Rooij, S.R., Roseboom, T.J., Nathanielsz, P.W., Witte, O.W., Schwab, M., 2017b. Effects of prenatal stress on structural brain development and aging in humans. Neurosci. Biobehav. Rev (this issue).

Frasch, M.G., Muller, T., Wicher, C., Weiss, C., Lohle, M., Schwab, K., et al., 2007. Fetal body weight and the development of the control of the cardiovascular system in fetal sheep. J. Physiol. 579, 893–907.

Frodl, T., O'Keane, V., 2013. How does the brain deal with cumulative stress? A review with focus on developmental stress, HPA axis function and hippocampal structure in humans. Neurobiol. Dis. 52, 24–37.

Gabrieli, J.D., Ghosh, S.S., Whitfield-Gabrieli, S., 2015. Prediction as a humanitarian and pragmatic contribution from human cognitive neuroscience. Neuron 85, 11–26.

Gardner, M., Bann, D., Wiley, L., Cooper, R., Hardy, R., Nitsch, D., et al., 2014. Gender and telomere length: systematic review and meta-analysis. Exp. Gerontol. 51, 15–27.

Gaser, C., Franke, K., Kloppel, S., Koutsouleris, N., Sauer, H., Alzheimer's Disease Neuroimaging, I., 2013. *BrainAGE* in mild cognitive impaired patients: predicting the conversion to Alzheimer's disease. PLoS One 8, e67346.

Gibbs, W.W., 2014. Biomarkers and ageing: the clock-watcher. Nature 508, 168–170.

Gluckman, P.D., Hanson, M.A., Cooper, C., Thornburg, K.L., 2008. Effect of in utero and early-life conditions on adult health and disease. N. Engl. J. Med. 359, 61–73.

Gomes, N.M., Ryder, O.A., Houck, M.L., Charter, S.J., Walker, W., Forsyth, N.R., et al., 2011. Comparative biology of mammalian telomeres: hypotheses on ancestral states and the roles of telomeres in longevity determination. Aging Cell 10, 761–768.

Good, C.D., Johnsrude, I.S., Ashburner, J., Henson, R.N., Friston, K.J., Frackowiak, R.S., 2001. A voxel-based morphometric study of ageing in 465 normal adult human brains. Neuroimage 14, 21–36.

Griffiths, B.B., Hunter, R.G., 2014. Neuroepigenetics of stress. Neuroscience 275, 420–435.

Groves, A.R., Smith, S.M., Fjell, A.M., Tamnes, C.K., Walhovd, K.B., Douaud, G., et al., 2012. Benefits of multi-modal fusion analysis on a large-scale dataset: life-span patterns of inter-subject variability in cortical morphometry and white matter microstructure. Neuroimage 63, 365–380.

Habekost, T., Vogel, A., Rostrup, E., Bundesen, C., Kyllingsbaek, S., Garde, E., et al., 2013. Visual processing speed in old age. Scand. J. Psychol. 54, 89–94.

Habekost, T., 2015. Clinical TVA-based studies: a general review. Front. Psychol. 6, 290.

Habes, M., Janowitz, D., Erus, G., Toledo, J.B., Resnick, S.M., Doshi, J., et al., 2016. Advanced brain aging: relationship with epidemiologic and genetic risk factors, and overlap with Alzheimer disease atrophy patterns. Transl. Psychiatry 6, e775.

Han, C.E., Peraza, L.R., Taylor, J.P., Kaiser, M., 2014. Predicting age across human lifespan based on structural connectivity from diffusion tensor imaging, IEEE Biomedical Circuits and Systems Conference (BioCAS) Proceedings. Lausanne 137–140.

Hannum, G., Guinney, J., Zhao, L., Zhang, L., Hughes, G., Sadda, S., et al., 2013. Genome-wide methylation profiles reveal quantitative views of human aging rates. Mol. Cell 49, 359–367.

Harris, A., Seckl, J., 2011. Glucocorticoids, prenatal stress and the programming of disease. Horm. Behav. 59, 279–289.

Hawkins, P., Steyn, C., McGarrigle, H.H., Saito, T., Ozaki, T., Stratford, L.L., et al., 1999. Effect of maternal nutrient restriction in early gestation on development of the hypothalamic-pituitary-adrenal axis in fetal sheep at 0.8–0.9 of gestation. J. Endocrinol. 163, 553–561.

Haycock, P.C., Heydon, E.E., Kaptoge, S., Butterworth, A.S., Thompson, A., Willeit, P., 2014. Leucocyte telomere length and risk of cardiovascular disease: systematic review and meta-analysis. BMJ 349, g4227.

Hedden, T., Gabrieli, J.D.E., 2004. Insights into the ageing mind: a view from cognitive neuroscience. Nat. Rev. Neurosci. 5, 87–96.

Henje Blom, E., Han, L.K., Connolly, C.G., Ho, T.C., Lin, J., LeWinn, K.Z., et al., 2015. Peripheral telomere length and hippocampal volume in adolescents with major depressive disorder. Transl. Psychiatry 5, e676.

Hogstrom, L.J., Westlye, L.T., Walhovd, K.B., Fjell, A.M., 2013. The structure of the cerebral cortex across adult life: age-related patterns of surface area, thickness, and gyrification. Cereb. Cortex 23, 2521–2530.

Horn, J.L., Cattell, R.B., 1967. Age differences in fluid and crystallized intelligence. Acta Psychol. 26, 107–129.

Horvath, S., Levine, A.J., 2015. HIV-1 infection accelerates age according to the epigenetic clock. J. Infect. Dis. 212, 1563–1573.

Horvath, S., Ritz, B.R., 2015. Increased epigenetic age and granulocyte counts in the blood of Parkinson's disease patients. Aging (Albany NY) 7, 1130–1142.

Horvath, S., Erhart, W., Brosch, M., Ammerpohl, O., von Schonfels, W., Ahrens, M., et al., 2014. Obesity accelerates epigenetic aging of human liver. Proc. Natl. Acad. Sci. U. S. A. 111, 15538–15543.

Horvath, S., Garagnani, P., Bacalini, M.G., Pirazzini, C., Salvioli, S., Gentilini, D., et al., 2015. Accelerated epigenetic aging in Down syndrome. Aging Cell 14, 491–495.

Horvath, S., Gurven, M., Levine, M.E., Trumble, B.C., Kaplan, H., Allayee, H., et al., 2016a. An epigenetic clock analysis of race/ethnicity, sex, and coronary heart disease. Genome Biol. 17, 171.

Horvath, S., Langfelder, P., Kwak, S., Aaronson, J., Rosinski, J., Vogt, T.F., et al., 2016b. Huntington's disease accelerates epigenetic aging of human brain and disrupts DNA methylation levels. Aging (Albany NY) 8, 1485–1512.

Horvath, S., 2013. DNA methylation age of human tissues and cell types. Genome Biol. 14, R115.

Hoyer, D., Heinicke, E., Jaekel, S., Tetschk, F., Di Pietro Paolo, D., Haueisen, J., et al., 2009. Indices of fetal development derived from heart rate patterns. Early Hum. Dev. 85, 379–386.

Hoyer, D., Tetschke, F., Jaekel, S., Nowack, S., Witte, O.W., Schleussner, E., Schneider, U., 2013. Fetal functional brain age assessed from universal developmental indices obtained from neuro-vegetative activity patterns. PLoS One 8, e74431.

Hoyer, D., Kowalski, E.M., Schmidt, A., Tetschke, F., Nowack, S., Rudolph, A., et al., 2014. Fetal autonomic brain age scores, segmented heart rate variability analysis, and traditional short term variability. Front. Hum. Neurosci. 8, 948.

Hoyer, D., Schneider, U., Kowalski, E.M., Schmidt, A., Witte, O.W., Schleussner, E., et al., 2015. Validation of functional fetal autonomic brain age score fABAS in 5 min short recordings. Physiol. Meas. 36, 2369–2378.

Hoyer, D., Zebrowski, J., Cysarz, D., Goncalves, H., Pytlik, A., Amorim-Costa, C., et al., 2017. Monitoring fetal maturation-objectives, techniques and indices of autonomic function. Physiol. Meas. 38, R61–R88.

Huda, N., Tanaka, H., Herbert, B.S., Reed, T., Gilley, D., 2007. Shared environmental factors associated with telomere length maintenance in elderly male twins. Aging Cell 6, 709–713.

Insel, K.C., Merkle, C.J., Hsiao, C.P., Vidrine, A.N., Montgomery, D.W., 2012. Biomarkers for cognitive aging part I: telomere length, blood pressure and cognition among individuals with hypertension. Biol. Res. Nurs. 14, 124–132.

Jacobs, E.G., Epel, E.S., Lin, J., Blackburn, E.H., Rasgon, N.L., 2014. Relationship between leukocyte telomere length, telomerase activity, and hippocampal volume in early aging. JAMA Neurol. 71, 921–923.

Jenkins, E.C., Velinov, M.T., Ye, L., Gu, H., Li, S., Jenkins Jr., E.C., et al., 2006. Telomere shortening in T lymphocytes of older individuals with Down syndrome and dementia. Neurobiol. Aging 27, 941–945.

Jones, D.K., Cercignani, M., 2010. Twenty-five pitfalls in the analysis of diffusion MRI data. NMR Biomed. 23, 803–820.

Jones, D.K., Knosche, T.R., Turner, R., 2013. White matter integrity, fiber count, and other fallacies: the do's and don'ts of diffusion MRI. Neuroimage 73, 239–254.

Jung, R.E., Haier, R.J., 2007. The parieto-Frontal integration theory (P-FIT) of intelligence: converging neuroimaging evidence. Behav. Brain Sci. 30, 135–154 discussion 154–187.

Jylhava, J., Pedersen, N.L., Hagg, S., 2017. Biological age predictors. EBioMedicine 21, 29–36.

Kananen, L., Surakka, I., Pirkola, S., Suvisaari, J., Lonnqvist, J., Peltonen, L., et al., 2010. Childhood adversities are associated with shorter telomere length at adult age both in individuals with an anxiety disorder and controls. PLoS One 5, e10826.

Kandel, B.M., Wolk, D.A., Gee, J.C., Avants, B., 2013. Predicting cognitive data from medical images using sparse linear regression. Inf. Process. Med. Imaging 23, 86–97.

Kanwisher, N., 2010. Functional specificity in the human brain: a window into the functional architecture of the mind. Proc. Natl. Acad. Sci. U. S. A. 107, 11163–11170.

Kauffman, S.A., 1993. The Origins of Order: Self-Organization and Selection in Evolution. Oxford University Press, Oxford, New York.

Khundrakpam, B.S., Tohka, J., Evans, A.C., Development, Brain, Cooperative, G., 2015. Prediction of brain maturity based on cortical thickness at different spatial resolutions. Neuroimage 111, 350–359.

Kiefer, I., Siegel, E., Preissl, H., Ware, M., Schauf, B., Lowery, C., Eswaran, H., 2008. Delayed maturation of auditory-evoked responses in growth-restricted fetuses revealed by magnetoencephalographic recordings. Am. J. Obstet. Gynecol. 199 (50), e501–507.

King, K.S., Kozlitina, J., Rosenberg, R.N., Peshock, R.M., McColl, R.W., Garcia, C.K., 2014. Effect of leukocyte telomere length on total and regional brain volumes in a large population-based cohort. JAMA Neurol. 71, 1247–1254.

Knoops, A.J., Gerritsen, L., van der Graaf, Y., Mali, W.P., Geerlings, M.I., 2012. Loss of entorhinal cortex and hippocampal volumes compared to whole brain volume in normal aging: the SMART-Medea study. Psychiatry Res. 203, 31–37.

Koehl, M., Lemaire, V., Le Moal, M., Abrous, D.N., 2009. Age-dependent effect of prenatal stress on hippocampal cell proliferation in female rats. Eur. J. Neurosci. 29, 635–640.

Kong, C.M., Lee, X.W., Wang, X., 2013. Telomere shortening in human diseases. FEBS J. 280, 3180–3193.

Konukoglu, E., Glocker, B., Zikic, D., Criminisi, A., 2013. Neighbourhood approximation using randomized forests. Med. Image Anal. 17, 790–804.

Kouskouti, C., Regner, K., Knabl, J., Kainer, F., 2017. Cardiotocography and the evolution into computerised cardiotocography in the management of intrauterine growth restriction. Arch. Gynecol. Obstet. 295, 811–816.

Koutsouleris, N., Davatzikos, C., Borgwardt, S., Gaser, C., Bottlender, R., Frodl, T., et al., 2014. Accelerated brain aging in schizophrenia and beyond: a neuroanatomical marker of psychiatric disorders. Schizophr. Bull. 40, 1140–1153.

Kyllingsbaek, S., 2006. Modeling visual attention. Behav. Res. Methods 38, 123–133.

Lapham, K., Kvale, M.N., Lin, J., Connell, S., Croen, L.A., Dispensa, B.P., et al., 2015. Automated assay of telomere length measurement and informatics for 100, 000 subjects in the genetic epidemiology research on adult health and aging (GERA) cohort. Genetics 200, 1061–1072.

Laplante, M., Sabatini, D.M., 2012. mTOR signaling in growth control and disease. Cell 149, 274–293.

Levine, M.E., Lu, A.T., Bennett, D.A., Horvath, S., 2015. Epigenetic age of the pre-frontal cortex is associated with neuritic plaques, amyloid load, and Alzheimer's disease related cognitive functioning. Aging (Albany NY) 7, 1198–1211.

Liem, F., Varoquaux, G., Kynast, J., Beyer, F., Kharabian Masouleh, S., Huntenburg, J.M., et al., 2017. Predicting brain-age from multimodal imaging data captures cognitive impairment. Neuroimage 148, 179–188.

Lin, L., Jin, C., Fu, Z., Zhang, B., Bin, G., Wu, S., 2016. Predicting healthy older adult's brain age based on structural connectivity networks using artificial neural networks. Comput. Methods Programs Biomed. 125, 8–17.

Lindqvist, D., Epel, E.S., Mellon, S.H., Penninx, B.W., Revesz, D., Verhoeven, J.E., et al., 2015. Psychiatric disorders and leukocyte telomere length: underlying mechanisms linking mental illness with cellular aging. Neurosci. Biobehav. Rev. 55, 333–364.

Liu, J.P., 2014. Molecular mechanisms of ageing and related diseases. Clin. Exp. Pharmacol. Physiol. 41, 445–458.

Lopez-Otin, C., Blasco, M.A., Partridge, L., Serrano, M., Kroemer, G., 2013. The hallmarks of aging. Cell 153, 1194–1217.

Lowe, D., Horvath, S., Raj, K., 2016. Epigenetic clock analyses of cellular senescence and ageing. Oncotarget 7, 8524–8531.

Lowsky, D.J., Olshansky, S.J., Bhattacharya, J., Goldman, D.P., 2014. Heterogeneity in healthy aging. J. Gerontol. A Biol. Sci. Med. Sci. 69, 640–649.

Luck, S.J., Vogel, E.K., 2013. Visual working memory capacity: from psychophysics and neurobiology to individual differences. Trends Cogn. Sci. 17, 391–400.

Luders, E., Cherbuin, N., Gaser, C., 2016. Estimating brain age using high-resolution pattern recognition: younger brains in long-term meditation practitioners. Neuroimage 134, 508–513.

Lukens, J.N., Van Deerlin, V., Clark, C.M., Xie, S.X., Johnson, F.B., 2009. Comparisons of telomere lengths in peripheral blood and cerebellum in Alzheimer's disease. Alzheimers Dement. 5, 463–469.

Malter Cohen, M., Jing, D., Yang, R.R., Tottenham, N., Lee, F.S., Casey, B.J., 2013. Early-life stress has persistent effects on amygdala function and development in mice and humans. Proc. Natl. Acad. Sci. U. S. A. 110, 18274–18278.

Mamdani, F., Rollins, B., Morgan, L., Myers, R.M., Barchas, J.D., Schatzberg, A.F., et al., 2015. Variable telomere length across post-mortem human brain regions and specific reduction in the hippocampus of major depressive disorder. Transl. Psychiatry 5, e636.

Marchetto, N.M., Glynn, R.A., Ferry, M.L., Ostojic, M., Wolff, S.M., Yao, R., Haussmann, M.F., 2016. Prenatal stress and newborn telomere length. Am. J. Obstet. Gynecol. 215 (9), e91–98.

Marioni, R.E., Shah, S., McRae, A.F., Chen, B.H., Colicino, E., Harris, S.E., et al., 2015a. DNA methylation age of blood predicts all-cause mortality in later life. Genome Biol. 16, 25.

Marioni, R.E., Shah, S., McRae, A.F., Ritchie, S.J., Muniz-Terrera, G., Harris, S.E., et al., 2015b. The epigenetic clock is correlated with physical and cognitive fitness in the Lothian Birth Cohort 1936. Int. J. Epidemiol. 44, 1388–1396.

Marioni, R.E., Harris, S.E., Shah, S., McRae, A.F., von Zglinicki, T., Martin-Ruiz, C., et al., 2016. The epigenetic clock and telomere length are independently associated with chronological age and mortality. Int. J. Epidemiol pii: dyw041. [Epub ahead of print] PubMed PMID: 27075770; PubMed Central PMCID: PMC4864882.

Mather, K.A., Jorm, A.F., Parslow, R.A., Christensen, H., 2011. Is telomere length a biomarker of aging? A review. J. Gerontol. A Biol. Sci. Med. Sci. 66, 202–213.

McAvinue, L.P., Habekost, T., Johnson, K.A., Kyllingsbaek, S., Vangkilde, S., Bundesen, C., Robertson, I.H., 2012. Sustained attention, attentional selectivity, and attentional capacity across the lifespan. Atten. Percept. Psychophys. 74, 1570–1582.

Muezzinler, A., Zaineddin, A.K., Brenner, H., 2013. A systematic review of leukocyte telomere length and age in adults. Ageing Res. Rev. 12, 509–519.

Mutsaers, H.A., Tofighi, R., 2012. Dexamethasone enhances oxidative stress-induced cell death in murine neural stem cells. Neurotox. Res. 22, 127–137.

Mwangi, B., Hasan, K.M., Soares, J.C., 2013. Prediction of individual subject's age across the human lifespan using diffusion tensor imaging: a machine learning approach. Neuroimage 75, 58–67.

Naess, A.B., Kirkengen, A.L., 2015. Is childhood stress associated with shorter telomeres? Tidsskr. Nor. Laegeforen. 135, 1356–1360.

Neeb, H., Zilles, K., Shah, N.J., 2006. Fully-automated detection of cerebral water content changes: study of age- and gender-related H2O patterns with quantitative MRI. Neuroimage 29, 910–922.

Needham, B.L., Mezuk, B., Bareis, N., Lin, J., Blackburn, E.H., Epel, E.S., 2015a. Depression, anxiety and telomere length in young adults: evidence from the National Health and Nutrition Examination Survey. Mol. Psychiatry 20, 520–528.

Needham, B.L., Rehkopf, D., Adler, N., Gregorich, S., Lin, J., Blackburn, E.H., Epel, E.S., 2015b. Leukocyte telomere length and mortality in the National Health and Nutrition Examination Survey, 1999–2002. Epidemiology 26, 528–535.

Negron-Oyarzo, I., Lara-Vasquez, A., Palacios-Garcia, I., Fuentealba, P., Aboitiz, F., 2016. Schizophrenia and reelin: a model based on prenatal stress to study epigenetics, brain development and behavior. Biol. Res. 49, 16.

Nicolis, G., Prigogine, I., 1977. Self-organization in Nonequilibrum Systems: from Dissipative Structures to Order Through Fluctuations. Wiley, New York u.a.

Nijhuis, J.G., Prechtl, H.F., Martin Jr., C.B., Bots, R.S., 1982. Are there behavioural states in the human fetus? Early Hum. Dev. 6, 177–195.

Nijhuis, I.J., ten Hof, J., Mulder, E.J., Nijhuis, J.G., Narayan, H., Taylor, D.J., Visser, G.H., 2000. Fetal heart rate in relation to its variation in normal and growth retarded fetuses. Eur. J. Obstet. Gynecol. Reprod. Biol. 89, 27–33.

Nijland, M.J., Mitsuya, K., Li, C., Ford, S., McDonald, T.J., Nathanielsz, P.W., Cox, L.A., 2010. Epigenetic modification of fetal baboon hepatic phosphoenolpyruvate carboxykinase following exposure to moderately reduced nutrient availability. J. Physiol. 588, 1349–1359.

Nilsonne, G., Tamm, S., Mansson, K.N., Akerstedt, T., Lekander, M., 2015. Leukocyte telomere length and hippocampus volume: a meta-analysis. F1000Res 4, 1073.

Njajou, O.T., Hsueh, W.C., Blackburn, E.H., Newman, A.B., Wu, S.H., Li, R., et al., 2009. Association between telomere length, specific causes of death, and years of healthy life in health, aging, and body composition, a population-based cohort study. J. Gerontol. A Biol. Sci. Med. Sci. 64, 860–864.

Nordfjall, K., Larefalk, A., Lindgren, P., Holmberg, D., Roos, G., 2005. Telomere length and heredity: indications of paternal inheritance. Proc. Natl. Acad. Sci. U. S. A. 102, 16374–16378.

O'Donovan, A., Tomiyama, A.J., Lin, J., Puterman, E., Adler, N.E., Kemeny, M., et al., 2012. Stress appraisals and cellular aging: a key role for anticipatory threat in the relationship between psychological stress and telomere length. Brain Behav. Immun. 26, 573–579.

Pardoe, H.R., Cole, J.H., Blackmon, K., Thesen, T., Kuzniecky, R., Human Epilepsy Project, I., 2017. Structural brain changes in medically refractory focal epilepsy resemble premature brain aging. Epilepsy Res. 133, 28–32.

Pardon, M.C., Rattray, I., 2008. What do we know about the long-term consequences of stress on ageing and the progression of age-related neurodegenerative disorders? Neurosci. Biobehav. Rev. 32, 1103–1120.

Pavanello, S., Hoxha, M., Dioni, L., Bertazzi, P.A., Snenghi, R., Nalesso, A., et al., 2011. Shortened telomeres in individuals with abuse in alcohol consumption. Int. J. Cancer 129, 983–992.

Pellegrini, L., Wetzel, A., Granno, S., Heaton, G., Harvey, K., 2017. Back to the tubule: microtubule dynamics in Parkinson's disease. Cell. Mol. Life Sci. 74, 409–434.

Penazzi, L., Bakota, L., Brandt, R., 2016. Microtubule dynamics in neuronal development, plasticity, and neurodegeneration. Int. Rev. Cell Mol. Biol. 321, 89–169.

Perna, L., Zhang, Y., Mons, U., Holleczek, B., Saum, K.U., Brenner, H., 2016. Epigenetic age acceleration predicts cancer, cardiovascular, and all-cause mortality in a German case cohort. Clin. Epigenet. 8, 64.

Petersen, S.E., Posner, M.I., 2012. The attention system of the human brain: 20 years after. Annu. Rev. Neurosci. 35, 73–89.

Pillai, M., James, D., 1990. The development of fetal heart rate patterns during normal pregnancy. Obstet. Gynecol. 76, 812–816.

Prescott, J., Kraft, P., Chasman, D.I., Savage, S.A., Mirabello, L., Berndt, S.I., et al., 2011. Genome-wide association study of relative telomere length. PLoS One 6, e19635.

Provenzi, L., Giorda, R., Beri, S., Montirosso, R., 2016. SLC6A4 methylation as an epigenetic marker of life adversity exposures in humans: a systematic review of literature. Neurosci. Biobehav. Rev. 71, 7–20.

Ptak, R., 2012. The frontoparietal attention network of the human brain: action, saliency, and a priority map of the environment. Neuroscientist: Rev. J. Bringing Neurobiol. Neurol. Psychiatry 18, 502–515.

Puterman, E., Gemmill, A., Karasek, D., Weir, D., Adler, N.E., Prather, A.A., Epel, E.S., 2016. Lifespan adversity and later adulthood telomere length in the nationally representative US Health and Retirement Study. Proc. Natl. Acad. Sci. U. S. A. 113, E6335–E6342.

Puvill, T., Lindenberg, J., de Craen, A.J., Slaets, J.P., Westendorp, R.G., 2016. Impact of physical and mental health on life satisfaction in old age: a population based observational study. BMC Geriatr. 16, 194.

Qiu, A., Rifkin-Graboi, A., Chen, H., Chong, Y.S., Kwek, K., Gluckman, P.D., et al., 2013. Maternal anxiety and infants' hippocampal development: timing matters. Transl. Psychiatry 3, e306.

Quach, A., Levine, M.E., Tanaka, T., Lu, A.T., Chen, B.H., Ferrucci, L., et al., 2017. Epigenetic clock analysis of diet, exercise, education, and lifestyle factors. Aging (Albany NY) 9, 419–446.

Rakers, F., Frauendorf, V., Rupprecht, S., Schiffner, R., Bischoff, S.J., Kiehntopf, M., et al., 2013. Effects of early- and late-gestational maternal stress and synthetic glucocorticoid on development of the fetal hypothalamus-pituitary-adrenal axis in sheep. Stress 16, 122–129.

Rando, T.A., Chang, H.Y., 2012. Aging, rejuvenation, and epigenetic reprogramming: resetting the aging clock. Cell 148, 46–57.

Raz, N., Rodrigue, K.M., 2006. Differential aging of the brain: patterns, cognitive correlates and modifiers. Neurosci. Biobehav. Rev. 30, 730–748.

Resnick, S.M., Pham, D.L., Kraut, M.A., Zonderman, A.B., Davatzikos, C., 2003. Longitudinal magnetic resonance imaging studies of older adults: a shrinking brain. J. Neurosci. 23, 3295–3301.

Ritchie, S.J., Tucker-Drob, E.M., Deary, I.J., 2014. A strong link between speed of visual discrimination and cognitive ageing. Curr. Biol. 24, R681–683.

Rizvi, S., Raza, S.T., Mahdi, F., 2014. Telomere length variations in aging and age-related diseases. Curr. Aging Sci. 7, 161–167.

Rizzo, L.B., Costa, L.G., Mansur, R.B., Swardfager, W., Belangero, S.I., Grassi-Oliveira, R., et al., 2014a. The theory of bipolar disorder as an illness of accelerated aging: implications for clinical care and research. Neurosci. Biobehav. Rev. 42, 157–169.

Rizzo, V., Richman, J., Puthanveettil, S.V., 2014b. Dissecting mechanisms of brain aging by studying the intrinsic excitability of neurons. Front. Aging Neurosci. 6, 337.

Rode, L., Nordestgaard, B.G., Bojesen, S.E., 2015. Peripheral blood leukocyte telomere length and mortality among 64,637 individuals from the general population. J. Natl. Cancer Inst. 107, djv074.

Rose'meyer, R., 2013. A review of the serotonin transporter and prenatal cortisol in the development of autism spectrum disorders. Mol. Autism 4, 37.

Rossiello, F., Herbig, U., Longhese, M.P., Fumagalli, M., d'Adda di Fagagna, F., 2014. Irreparable telomeric DNA damage and persistent DDR signalling as a shared causative mechanism of cellular senescence and ageing. Curr. Opin. Genet. Dev. 26, 89–95.

Rotar, O., Moguchaia, E., Boyarinova, M., Kolesova, E., Khromova, N., Freylikhman, O., et al., 2015. Seventy years after the siege of Leningrad: does early life famine still affect cardiovascular risk and aging? J. Hypertens. 33, 1772–1779 discussion 1779.

Sabuncu, M.R., Van Leemput, K., 2011. The relevance voxel machine (RVoxM): a bayesian method for image-based prediction. Med. Image Comput. Comput. Assist. Interv. 14, 99–106.

Sabuncu, M.R., Van Leemput, K., Alzheimer's Disease Neuroimaging, I., 2012. The relevance voxel machine (RVoxM): a self-tuning Bayesian model for informative image-based prediction. IEEE Trans. Med. Imaging 31, 2290–2306.

Salthouse, T.A., 1996. The processing-speed theory of adult age differences in cognition. Psychol. Rev. 103, 403–428.

Sanders, J.L., Newman, A.B., 2013. Telomere length in epidemiology: a biomarker of aging, age-related disease, both, or neither? Epidemiol. Rev. 35, 112–131.

Scheinost, D., Sinha, R., Cross, S.N., Kwon, S.H., Sze, G., Constable, R.T., Ment, L.R., 2017. Does prenatal stress alter the developing connectome? Pediatr. Res. 81, 214–226.

Scheller Madrid, A., Rode, L., Nordestgaard, B.G., Bojesen, S.E., 2016. Short telomere length and ischemic heart disease: observational and genetic studies in 290 022 individuals. Clin. Chem. 62, 1140–1149.

Schnack, H.G., van Haren, N.E., Nieuwenhuis, M., Hulshoff Pol, H.E., Cahn, W., Kahn, R.S., 2016. Accelerated brain aging in Schizophrenia: a longitudinal pattern recognition study. Am. J. Psychiatry 173, 607–616.

Schwab, M., Antonow-Schlorke, I., Kuhn, B., Muller, T., Schubert, H., Walter, B., et al., 2001. Effect of antenatal betamethasone treatment on microtubule-associated proteins MAP1 B and MAP2 in fetal sheep. J. Physiol. 530, 497–506.

Shalev, I., Moffitt, T.E., Sugden, K., Williams, B., Houts, R.M., Danese, A., et al., 2013. Exposure to violence during childhood is associated with telomere erosion from 5 to 10 years of age: a longitudinal study. Mol. Psychiatry 18, 576–581.

Shaltout, H.A., Chappell, M.C., Rose, J.C., Diz, D.I., 2011. Exaggerated sympathetic mediated responses to behavioral or pharmacological challenges following antenatal betamethasone exposure. Am. J. Physiol. Endocrinol. Metab. 300, E979–985.

Shea, T.B., Rogers, E., Ashline, D., Ortiz, D., Sheu, M.S., 2002. Apolipoprotein E deficiency promotes increased oxidative stress and compensatory increases in antioxidants in brain tissue. Free Radic. Biol. Med. 33, 1115–1120.

Silk, T.J., Wood, A.G., 2011. Lessons about neurodevelopment from anatomical magnetic resonance imaging. J. Dev. Behav. Pediatr. 32, 158–168.

Simmons, R.A., 2012. Developmental origins of diabetes: the role of oxidative stress. Best Pract. Res. Clin. Endocrinol. Metab. 26, 701–708.

Sodhi, S.K., Linder, J., Chenard, C.A., Miller del, D., Haynes, W.G., Fiedorowicz, J.G., 2012. Evidence for accelerated vascular aging in bipolar disorder. J. Psychosom. Res. 73, 175–179.

Spearman, C., 1904. General intelligence, objectively determined and measured. Am. J. Psychol. 15, 201–292.

Sprott, R.L., 2010. Biomarkers of aging and disease: introduction and definitions. Exp. Gerontol. 45, 2–4.

Starnawska, A., Tan, Q., Lenart, A., McGue, M., Mors, O., Borglum, A.D., et al., 2017. Blood DNA methylation age is not associated with cognitive functioning in middle-aged monozygotic twins. Neurobiol. Aging 50, 60–63.

Steffener, J., Habeck, C., O'Shea, D., Razlighi, Q., Bherer, L., Stern, Y., 2016. Differences between chronological and brain age are related to education and self-reported physical activity. Neurobiol. Aging 40, 138–144.

Storsve, A.B., Fjell, A.M., Tamnes, C.K., Westlye, L.T., Overbye, K., Aasland, H.W., Walhovd, K.B., 2014. Differential longitudinal changes in cortical thickness, surface area and volume across the adult life span: regions of accelerating and decelerating

change. J. Neurosci. 34, 8488–8498.

Svenson, U., Nordfjall, K., Baird, D., Roger, L., Osterman, P., Hellenius, M.L., Roos, G., 2011. Blood cell telomere length is a dynamic feature. PLoS One 6, e21485.

Szebeni, A., Szebeni, K., DiPeri, T., Chandley, M.J., Crawford, J.D., Stockmeier, C.A., Ordway, G.A., 2014. Shortened telomere length in white matter oligodendrocytes in major depression: potential role of oxidative stress. Int. J. Neuropsychopharmacol. 17, 1579–1589.

Tacutu, R., Budovsky, A., Yanai, H., Fraifeld, V.E., 2011. Molecular links between cellular senescence, longevity and age-related diseases – a systems biology perspective. Aging (Albany NY) 3, 1178–1191.

Takata, Y., Kikukawa, M., Hanyu, H., Koyama, S., Shimizu, S., Umahara, T., et al., 2012. Association between ApoE phenotypes and telomere erosion in Alzheimer's disease. J. Gerontol. A Biol. Sci. Med. Sci. 67, 330–335.

Takubo, K., Izumiyama-Shimomura, N., Honma, N., Sawabe, M., Arai, T., Kato, M., et al., 2002. Telomere lengths are characteristic in each human individual. Exp. Gerontol. 37, 523–531.

Takubo, K., Aida, J., Izumiyama-Shimomura, N., Ishikawa, N., Sawabe, M., Kurabayashi, R., et al., 2010. Changes of telomere length with aging. Geriatr. Gerontol. Int. 10 (Suppl. 1), S197–206.

Tansey, M.G., Goldberg, M.S., 2010. Neuroinflammation in Parkinson's disease: its role in neuronal death and implications for therapeutic intervention. Neurobiol. Dis. 37, 510–518.

Tarry-Adkins, J.L., Ozanne, S.E., 2014. The impact of early nutrition on the ageing trajectory. Proc. Nutr. Soc. 73, 289–301.

Terribilli, D., Schaufelberger, M.S., Duran, F.L., Zanetti, M.V., Curiati, P.K., Menezes, P.R., et al., 2011. Age-related gray matter volume changes in the brain during non-elderly adulthood. Neurobiol. Aging 32, 354–368.

Thayer, J.F., Ahs, F., Fredrikson, M., Sollers 3rd, J.J., Wager, T.D., 2012. A meta-analysis of heart rate variability and neuroimaging studies: implications for heart rate variability as a marker of stress and health. Neurosci. Biobehav. Rev. 36, 747–756.

Thomas, P., Nj, O.C., Fenech, M., 2008. Telomere length in white blood cells, buccal cells and brain tissue and its variation with ageing and Alzheimer's disease. Mech. Ageing Dev. 129, 183–190.

Tian, L., Ma, L., Wang, L., 2016. Alterations of functional connectivities from early to middle adulthood: clues from multivariate pattern analysis of resting-state fMRI data. Neuroimage 129, 389–400.

Tournier, J.D., Mori, S., Leemans, A., 2011. Diffusion tensor imaging and beyond. Magn. Reson. Med. 65, 1532–1556.

Valdes, A.M., Deary, I.J., Gardner, J., Kimura, M., Lu, X., Spector, T.D., et al., 2010. Leukocyte telomere length is associated with cognitive performance in healthy women. Neurobiol. Aging 31, 986–992.

van den Bergh, B.R.H., van den Heuvel, M.I., Lahti, M., Braeken, M., de Rooij, S.R., Entringer, S., et al., 2017. Prenatal developmental origins of behavior and mental health: the influence of maternal stress in pregnancy. Neurosci. Biobehav. Rev this issue.

Van Hecke, W., Emsell, L., Sunaert, S., 2015. Diffusion Tensor Imaging: a Practical Handbook. Springer, New York.

Van Leeuwen, P., Lange, S., Bettermann, H., Gronemeyer, D., Hatzmann, W., 1999. Fetal heart rate variability and complexity in the course of pregnancy. Early Hum. Dev. 54, 259–269.

Van Leeuwen, P., Geue, D., Lange, S., Hatzmann, W., Gronemeyer, D., 2003. Changes in the frequency power spectrum of fetal heart rate in the course of pregnancy. Prenat. Diagn. 23, 909–916.

Van den Bergh, B.R., 2011. Developmental programming of early brain and behaviour development and mental health: a conceptual framework. Dev. Med. Child Neurol. 53 (Suppl. 4), 19–23.

Varoquaux, G., Thirion, B., 2014. How machine learning is shaping cognitive neuroimaging. Gigascience 3, 28.

Ventriglio, A., Gentile, A., Baldessarini, R.J., Bellomo, A., 2015. Early-life stress and psychiatric disorders: epidemiology, neurobiology and innovative pharmacological targets. Curr. Pharm. Des. 21, 1379–1387.

Vivar, C., 2015. Adult hippocampal neurogenesis, aging and neurodegenerative diseases:

possible strategies to prevent cognitive impairment. Curr. Top. Med. Chem. 15, 2175–2192.

von Zglinicki, T., Martin-Ruiz, C.M., 2005. Telomeres as biomarkers for ageing and age-related diseases. Curr. Mol. Med. 5, 197–203.

Vos, T., Flaxman, A.D., Naghavi, M., Lozano, R., Michaud, C., Ezzati, M., et al., 2012. Years lived with disability (YLDs) for 1160 sequelae of 289 diseases and injuries 1990–2010: a systematic analysis for the Global Burden of Disease Study 2010. Lancet 380, 2163–2196.

Wang, B., Pham, T.D., 2011. MRI-based age prediction using hidden Markov models. J. Neurosci. Methods 199, 140–145.

Wang, J., Li, W., Miao, W., Dai, D., Hua, J., He, H., 2014. Age estimation using cortical surface pattern combining thickness with curvatures. Med. Biol. Eng. Comput. 52, 331–341.

Weischer, M., Bojesen, S.E., Cawthon, R.M., Freiberg, J.J., Tybjaerg-Hansen, A., Nordestgaard, B.G., 2012. Short telomere length, myocardial infarction, ischemic heart disease, and early death. Arterioscler. Thromb. Vasc. Biol. 32, 822–829.

Wentzensen, I.M., Mirabello, L., Pfeiffer, R.M., Savage, S.A., 2011. The association of telomere length and cancer: a meta-analysis. Cancer Epidemiol. Biomarkers Prev. 20, 1238–1250.

Wikgren, M., Karlsson, T., Lind, J., Nilbrink, T., Hultdin, J., Sleegers, K., et al., 2012. Longer leukocyte telomere length is associated with smaller hippocampal volume among non-demented APOE epsilon3/epsilon3 subjects. PLoS One 7, e34292.

Wikgren, M., Karlsson, T., Soderlund, H., Nordin, A., Roos, G., Nilsson, L.G., et al., 2014. Shorter telomere length is linked to brain atrophy and white matter hyperintensities. Age Ageing 43, 212–217.

Willeit, P., Raschenberger, J., Heydon, E.E., Tsimikas, S., Haun, M., Mayr, A., et al., 2014. Leucocyte telomere length and risk of type 2 diabetes mellitus: new prospective cohort study and literature-based meta-analysis. PLoS One 9, e112483.

Williams, S.E., Turley, C., Nettelbeck, T., Burns, N.R., 2009. A measure of inspection time in 4-year-old children: the Benny Bee IT task. Br. J Dev. Psychol. 27, 669–680.

Wilms, I.L., Nielsen, S., 2014. Normative perceptual estimates for 91 healthy subjects age 60–75: impact of age, education, employment, physical exercise, alcohol, and video gaming. Front. Psychol. 5, 1137.

Wood, J.M., Owsley, C., 2014. Useful field of view test. Gerontology 60, 315–318.

Wyrwoll, C.S., Holmes, M.C., 2012. Prenatal excess glucocorticoid exposure and adult affective disorders: a role for serotonergic and catecholamine pathways. Neuroendocrinology 95, 47–55.

Yang, Z., Ye, J., Li, C., Zhou, D., Shen, Q., Wu, J., et al., 2013. Drug addiction is associated with leukocyte telomere length. Sci. Rep. 3, 1542.

Yatham, L.N., Kapczinski, F., Andreazza, A.C., Trevor Young, L., Lam, R.W., Kauer-Sant'anna, M., 2009. Accelerated age-related decrease in brain-derived neurotrophic factor levels in bipolar disorder. Int. J. Neuropsychopharmacol. 12, 137–139.

Zekry, D., Herrmann, F.R., Irminger-Finger, I., Graf, C., Genet, C., Vitale, A.M., et al., 2010a. Telomere length and ApoE polymorphism in mild cognitive impairment, degenerative and vascular dementia. J. Neurol. Sci. 299, 108–111.

Zekry, D., Herrmann, F.R., Irminger-Finger, I., Ortolan, L., Genet, C., Vitale, A.M., et al., 2010b. Telomere length is not predictive of dementia or MCI conversion in the oldest old. Neurobiol. Aging 31, 719–720.

Zhang, D., Cheng, L., Craig, D.W., Redman, M., Liu, C., 2010. Cerebellar telomere length and psychiatric disorders. Behav. Genet. 40, 250–254.

Zhang, C.C., Xing, A., Tan, M.S., Tan, L., Yu, J.T., 2016. The role of MAPT in neurodegenerative diseases: genetics, mechanisms and therapy. Mol. Neurobiol. 53, 4893–4904.

Zheng, Y., Joyce, B.T., Colicino, E., Liu, L., Zhang, W., Dai, Q., et al., 2016. Blood epigenetic age may predict cancer incidence and mortality. EBioMedicine 5, 68–73.

Zhu, X., Han, W., Xue, W., Zou, Y., Xie, C., Du, J., Jin, G., 2016. The association between telomere length and cancer risk in population studies. Sci. Rep. 6, 22243.

Ziegler, G., Ridgway, G.R., Dahnke, R., Gaser, C., DiseaseAlzheimer's Disease Neuroimaging, I., 2014. Individualized Gaussian process-based prediction and detection of local and global gray matter abnormalities in elderly subjects. Neuroimage 97, 333–348.